

**UNIVERSIDADE FEDERAL DE MINAS GERAIS**

Programa de Pós-Graduação em Engenharia Metalúrgica, Materiais e de Minas

Marcos do Amaral Morais

**Bioacessibilidade no sistema digestivo/respiratório, determinação das fases e fontes de arsênio em partículas finas superficiais**

*“Gastric/lung bioaccessibility and identification of arsenic-bearing phases and sources of fine surface dust in a gold mining district.”*

Belo Horizonte

2019

Marcos do Amaral Morais

**Bioacessibilidade no sistema digestivo/respiratório, determinação das fases e fontes de arsênio em partículas finas superficiais**

*“Gastric/lung bioaccessibility and identification of arsenic-bearing phases and sources of fine surface dust in a gold mining district”*

**Versão Final**

Dissertação apresentada ao Programa Pós-Graduação em Engenharia Metalúrgica, Materiais e de Minas da Universidade Federal de Minas Gerais para obtenção do título de Mestre em Engenharia.

Orientadora: Prof<sup>a</sup>. Ph.D. Virginia S.T. Ciminelli

Coorientador: Massimo Gasparon

Belo Horizonte

2019

M827b

Morais, Marcos do Amaral.

Bioacessibilidade no sistema digestivo/respiratório, determinação das fases e fontes de arsênio em partículas finas superficiais [recurso eletrônico] / Marcos do Amaral Moraes. – 2019.

1 recurso online (68 f. : il., color.) : pdf.

Orientadora: Virginia Sampaio Teixeira Ciminelli.

Coorientador: Massimo Gasparon.

Dissertação (mestrado) - Universidade Federal de Minas Gerais, Escola de Engenharia.

Bibliografia: f. 57-68.

Exigências do sistema: Adobe Acrobat Reader.

1. Engenharia metalúrgica - Teses. 2. Arsênio – Teses. 3. Poeira em Minas – Teses. I. Ciminelli, Virginia Sampaio Teixeira. II. Gasparon, Massimo. III. Universidade Federal de Minas Gerais. Escola de Engenharia. IV. Título.

CDU: 669(043)

Ficha catalográfica: Biblioteca Prof. Mário Werneck, Escola de Engenharia da UFMG



UNIVERSIDADE FEDERAL DE MINAS GERAIS  
ESCOLA DE ENGENHARIA  
Programa de Pós-Graduação em Engenharia  
Metalúrgica, Materiais e de Minas



Dissertação intitulada "**Bioacessibilidade no Sistema Digestivo/respiratório, Determinação das Fases e Fontes de Arsênio em Partículas Finas Superficiais**", área de concentração: Tecnologia Mineral, apresentada pelo candidato **Marcos do Amaral Moraes**, para obtenção do grau de Mestre em Engenharia Metalúrgica, Materiais e de Minas, aprovada pela comissão examinadora constituída pelos seguintes membros:

Prof<sup>a</sup> Virginia Sampaio Teixeira Ciminelli  
Orientadora - Ph.D. (UFMG)

Prof<sup>a</sup> Mônica Cristina Teixeira  
Dr<sup>a</sup> (UFOP)

Prof. Júlio César José da Silva  
Dr. (UFJF)

Eng<sup>a</sup>. Cláudia Lima Caldeira  
Dr<sup>a</sup> (UFMG)

Prof. Rodrigo Lambert Oréfice  
Coordenador do Programa de Pós-Graduação em Engenharia  
Metalúrgica, Materiais e de Minas/UFMG

Belo Horizonte, 29 de março de 2019

## RESUMO

A exposição ao arsênio e os consequentes riscos para a saúde humana representam uma preocupação comum para as populações que vivem próximas a minerações de ouro que produzem resíduos contendo arsênio. Este é o caso de algumas regiões no Estado de Minas Gerais, Brasil. A bioacessibilidade (BAC) do arsênio em poeira inalável / *fine surface dust* (FSD, tamanho  $\leq 10 \mu\text{m}$ ) e amostras de poeira superficial (tamanho  $\leq 250 \mu\text{m}$ ) coletadas em uma região de mineração de ouro foi usada como ferramenta para determinar a fração de arsênio disponível (e.g., solúvel) em soluções simulando os fluidos de pulmão e gastrointestinal (GI). A BAC foi considerada baixa em ambos os ensaios (pulmão:  $2,7 \pm 1\%$ ,  $n = 5$  e G.I:  $3,4 \pm 2\%$ ,  $n = 14$ ) para amostras coletadas em área residencial. Um procedimento analítico foi desenvolvido para identificar as fases portadoras de arsênio e analisar os principais componentes que regulam a solubilidade do arsênio. Até cinco diferentes fases contendo de arsênio foram identificadas em um total de 35 constituintes identificados através de microscopia eletrônica de varredura com sistema de análise de imagens (*Mineral Liberation Analyzer - MLA*). Os oxi-hidróxidos de Fe e as denominadas “fases mistas” compreenderam as principais fases de arsênio encontradas nas amostras de poeira inalável, sendo assim responsáveis pela regulação da bioacessibilidade deste elemento. A microscopia eletrônica de transmissão mostrou que as “fases mistas” são uma mistura de agregados nanoestruturados formados por hematita e goethita entrelaçados com filossilicatos. As principais fases contendo As identificadas nas amostras de poeira inalável são similares àquelas relatadas em amostras de solo na mesma região. A fase predominante contendo arsênio encontrada no minério foi a arsenopirita, principalmente em partículas maiores ( $>10 \mu\text{m}$  de tamanho) o que, portanto, corrobora a sua rara ocorrência em poeiras residenciais. As contribuições da máxima exposição (ingresso) por meio de inalação e por ingestão são pequenas (0,1% e 5,2%, respectivamente) quando comparadas ao ingresso total de arsênio, considerando a ingestão de alimentos e de água. O ingresso total, por sua vez, é  $<7\%$  do limite inferior da dose de referência da Organização das Nações Unidas para Agricultura e Alimentação ( $\text{BMDL}_{0.5}$ ) de  $3,0 \mu\text{g}/\text{kg}$  de peso corporal/dia. Esses achados são originais, uma vez que se baseiam na identificação estatisticamente robusta de partículas individuais, e relevantes, ao esclarecer que a exposição por inalação ou ingestão de arsênio em região sob a influência da mineração de ouro pode ser classificada como de baixo risco.

Palavras-chave: Bioacessibilidade pulmonar. Bioacessibilidade gástrica/intestinal. Poeira inalável. Arsênio.

## ABSTRACT

Arsenic exposure and the consequent risks to human health, represents a common concern for populations living near gold mining operations producing arsenic-bearing wastes. This is the case of arsenic-rich gold mining districts in the State of Minas Gerais, Brazil. Arsenic bioaccessibility (BAC) in fine surface dust (FSD, particle size  $\leq 10 \mu\text{m}$ ) and surface dust samples (particle size  $\leq 250 \mu\text{m}$ ) collected from a gold mining district was used as a tool to determine the portion of arsenic that would be available via simulated lung and gastrointestinal (G.I) fluids. BAC was considered low for both tests (lung  $2.7 \pm 1\%$ ,  $n = 5$  and G.I  $3.4 \pm 2\%$ ,  $n = 14$  for residential surface dust samples). An analytical procedure was developed to further identify arsenic-bearing phases found in FSD samples and analyze the main components that regulate arsenic solubility. Up to five different arsenic-bearing phases were identified among a total of 35 minerals surveyed by scanning electron microscopy-based automated image analysis (Mineral Liberation Analyzer - MLA). Arsenic-bearing Fe oxy-hydroxides and mixed phases comprised the main arsenic phases encountered in FSD samples, thus likely being responsible for regulating arsenic bioaccessibility. Transmission electron microscopy showed that the mixed phases comprised a mix of oriented nanostructure aggregates formed by hematite and goethite entangled with phyllosilicates. The main As-bearing phases identified in FSD samples are similar to those reported in soil samples in the same region. The predominant arsenic-bearing phase encountered in the ore was arsenopyrite, mostly in large particles ( $>10 \mu\text{m}$  in size), and therefore unlikely to be found in residential dust. Arsenic intake from both inhalation and ingestion were minimal when compared to total arsenic intake (considering food and water ingestion), which itself was  $<7\%$  of the value established by the Food and Agriculture Organization of the United Nations Benchmark Dose Lower Confidence Limit (BMDL0.5) of  $3.0 \mu\text{g per kg}^{-1}$  body weight per day. These findings are relevant and clarify that the exposure from inhalation or ingestion of dust-related arsenic derived from the studied mining operation is likely to be minimal.

Keywords: Lung bioaccessibility. Gastric/Intestinal bioaccessibility. Surface dust. Arsenic.

## LIST OF FIGURES

Figure 3.1: Microregion Northwest where the studied site is located in the state of Minas Gerais, Brasil (highlighted in the inset). .....	23
Figure 3.2: Locations where the samples were collected in the town of Paracatu, the state of Minas Gerais, Brazil, and in the industrial site. ....	23
Figure 3.4: Photo of the physiologically based extraction test (PBET) apparatus containing the required enzyme. ....	25
Figure 4.1: Trace constituents of arsenic-bearing phases identified by MLA in the as-received ore (BP) sample and in the different size fractions (AsP: arsenopyrite; AsMx: As bearing mixed phases; AsFeOXH: As bearing Fe oxy-hydroxides). ....	43
Figure 4.2: Elemental concentrations determined by MLA and EDX (Al, Si), Leco (S) and ICP-OES (Fe, As) in BP samples.....	45
Figure 4.3: Elemental concentrations determined by MLA and EDX in FSD samples (H2 and H19). ....	45
Figure 4.4: Backscattered electron (BSE) images of mineralogical phases and elemental analyses (EDS) of main constituents of FSD* . ....	46
Figure 4.5: Transmission electron microscopy images of CP1 sample* .....	47
Figure 4.6: SAD analyses demonstrating the presence of hematite and goethite in CP1 sample. ....	48

## LIST OF TABLES

Table 2.1: Chemical composition of ALF (pH 4.5) (Wiseman, 2015).....	12
Table 2.2: Chemical composition of Gamble’s solutions (pH 7.4) (Boisa <i>et al.</i> , 2014) .....	13
Table 3.1: ICP-MS (Agilent 7500cs, Agilent Technologies Japan) instrument operational parameters.....	25
Table 3.2: Solid Liquid ratio used for bioaccessibility test.....	27
Table 3.3: Quality control data for arsenic analyses. ....	29
Table 3.4: Instrumental conditions (ICP-OES) .....	30
Table 3.5: SEM and MLA parameters.....	31
Table 4.1: Arsenic concentration and bioaccessible arsenic of surface dust samples collected in residential areas (fraction $\leq 250 \mu\text{m}$ ). ....	34
Table 4.2: Arsenic concentration and lung BAC in FSD samples ( $\leq 10 \mu\text{m}$ ). ....	35
Table 4.3: Main mineral phases weight (%) identified in FSD and BP samples by MLA analyses.....	40
Table 4.4: Trace constituents of sulfide and arsenic-bearing phases identified by MLA in FSD and BP samples.....	41
Table 4.5: Trace constituents of sulfide and arsenic-bearing phases identified by MLA in different sizes of BP samples.....	42
Table 4.6: Arsenic intake from surface dust and FSD.....	50



## LIST OF ABBREVIATIONS

ALF: artificial lysosomal fluid  
BAC: bioaccessibility  
BMDL<sub>0.5</sub>: benchmark dose lower confidence limit  
BSE: backscattered electron  
CDI: chemical daily intake  
CR: Carcinogenic Risk  
CSF: cancer slope factor  
EDS: energy dispersive X-ray spectrometry  
FSD: fine surface dust  
G.I: gastrointestinal  
HQ: hazard quotient  
HRA: health risk assessment  
HRTEM: high resolution transmission electron microscopy  
IARC: International Agency for Research on Cancer  
ICP-MS: inductively coupled plasma-mass spectrometry  
MLA: Mineral Liberation Analyzer  
NGO: non-governmental organization  
PBET: physiologically based extraction test  
PM: particulate matter  
RFD: reference doses  
SAD: selected area electron diffraction  
SBET: simple bioaccessibility extraction test  
SEM: scanning electron microscopy  
S/L: solid to liquid  
SLF: simulated lung fluid  
SRM: standard reference material  
STEM: scanning transmission electron microscopy  
TEM: transmission electron microscopy  
USEPA: United States Environmental Protection Agency  
WHO: World Health Organization

## CONSIDERAÇÕES INICIAIS

Embora a indústria de mineração esteja aprimorando as tecnologias utilizadas e, conseqüentemente, modernizando os controles ambientais, suas atividades são fontes potenciais de impacto ambiental na água, no solo e no ar. Nesse contexto, o escrutínio pela sociedade dos aspectos ambientais associados às atividades do setor vem aumentando gradativamente. Autoridades, organizações não-governamentais (ONGs) e associações comunitárias frequentemente se reúnem para compreender e debater a eficiência dos controles implementados para minimizar os impactos da indústria mineral. Vários aspectos são considerados nesses debates, porém, alguns são críticos e precisam ser bem abordados em profundidade.

O arsênio inorgânico é metaloide tóxico e classificado como carcinogênico (IARC, 2012), que pode estar naturalmente presente em depósitos de ouro. A exposição a minerais portadores de arsênio é motivo de grande preocupação para as partes interessadas e obriga o setor mineral a ter controles ambientais eficazes e de ser mais transparente em suas atividades. O arsênio é um elemento que ocorre naturalmente e é amplamente distribuído na crosta terrestre. Sua toxicidade ao ser humano depende de fatores geralmente associados à sua concentração e à exposição. Fontes de exposição ao arsênio no ar por exemplo, incluem a geração de material particulado e a ressuspensão de poeira. No entanto, as investigações associadas a alguns compostos específicos nas partículas de poeira, como o arsênio, ainda são limitadas. Além disso, estudos que quantificam a concentração de arsênio e investigam ainda a especiação do elemento em vários meios são de grande importância, pois permitem estimar melhor o risco à saúde humana (Guilherme *et al.*, 2012).

Estudos toxicológicos demonstraram que a fração solúvel de um contaminante é mais prejudicial à saúde do que a sua concentração total (Costa e Dreher, 1997; Ghio *et al.*, 1999; Adamson *et al.*, 2000; Prieditis e Adamson 2002; Heal *et al.*, 2005). Neste sentido, para avançar as avaliações sobre o potencial impacto ambiental causado pela mineração, várias ferramentas são necessárias, além dos ensaios tradicionais de caracterização de resíduos. Essas ferramentas incluem os ensaios de bioacessibilidade e biodisponibilidade (ensaios *in vitro* e *in vivo*).

O ensaio de biodisponibilidade é um procedimento usado para estimar a quantidade de um elemento que chega ao sistema circulatório a partir da sua absorção através do sistema digestivo ou pulmonar e requer o uso de animais vivos. Já os ensaios de bioacessibilidade medem a fração de um contaminante solúvel em fluídos similares ao do corpo humano e que, por consequência, encontra-se potencialmente disponível para ser absorvido. Estes ensaios são mais simples, menos custosos e não incluem o uso de animais.

O principal objetivo do presente trabalho foi gerar dados para a avaliação das contribuições de poeira de superfície (tamanho de partícula  $\leq 250 \mu\text{m}$ ) e poeira inalável / *fine surface dust* (FSD, fração  $\leq 10 \mu\text{m}$ ) para exposição total ao arsênio na cidade de Paracatu, Minas Gerais, utilizando ensaios de bioacessibilidade como ferramenta de avaliação de risco. O projeto teve ainda como objetivos, identificar as fontes e a distribuição de arsênio em amostras coletadas em áreas residenciais e operacionais da mineradora de ouro localizada na região de estudo. E, dessa forma, identificar os principais mecanismos que regulam a solubilidade do arsênio presente nas amostras de poeira em soluções similares ao fluido pulmonar.

# LIST OF CONTENTS

1	INTRODUCTION .....	1
2	LITERATURE REVIEW .....	3
2.1	Arsenic in Gold Mining Areas .....	3
2.2	Air Pollution and Particulate Matter .....	5
2.3	Bioavailability and Bioaccessibility.....	6
2.4	Bioaccessibility in gastrointestinal media .....	8
2.5	Bioaccessibility of Arsenic in Simulated Lung Fluids (SLF).....	10
2.6	Human Health Risk Assessment .....	17
2.7	Relevant Brazilian and International Legislation for arsenic in particulate matter 19	
3	MATERIALS AND METHODS .....	21
3.1	Studied site and sample collection / preparation.....	21
3.2	Experimental .....	24
3.2.1	Physiologically based extraction test (PBET) .....	24
3.2.2	BAC using simulated lung fluid (SLF).....	26
3.2.3	Elemental analysis in surface dust and FSD samples .....	27
3.2.4	Microscopy-based mineralogical quantification by Mineral Liberation Analyzer (MLA).....	30
3.2.5	Transmission electron microscopy (TEM) .....	32
3.2.6	RESULTS AND DISCUSSION .....	32
3.3	Gastrointestinal BAC .....	32
3.4	Lung BAC .....	35
3.5	Identification of main mineral phases and As-bearing phases.....	37
3.6	Health risk assessment (HRA) associated with As intake from inhalation and ingestion of FSD and surface dust .....	49
4	CONCLUSIONS .....	53
5	CONSIDERAÇÕES FINAIS .....	54
6	REFERENCES .....	56

## 1 INTRODUCTION

Mining activities can be potential sources of environmental pollution on water, soil, and air. Regarding soil and air media in particular, mining operations generate wastes that may influence large areas (Brotons *et al.*, 2010). Mining wastes and open mines are sources of fugitive dust, which in turn serves as an important pathway for metal (loid) transportation through the atmosphere. These materials can be deposited on soils and be re-suspended from settled dust (Jancsek-Turóczi *et al.*, 2013; Huang *et al.*, 2014b), thus favoring exposure by unintentional ingestion and inhalation.

Inorganic arsenic (As), a human carcinogenic element (IARC, 2012), constitutes one of the metalloids of concern associated with the mining of precious (e.g Au and Ag), base metals (e.g. Cu, Zn, Ni and Pb) and coal deposits. Yager *et al.* (2015) and Guney *et al.* (2016) reported that some elements including As, are highly toxic if exposed via inhalation, rendering it the importance to investigate the bioaccessibility (BAC) of this element to better quantify the exposure. Therefore, the use of simulated lung fluid (SLF), which has similarity to natural lung surfactant (Martin *et al.*, 2018), is required to extract elements of interest in BAC studies. Kastury *et al.* (2017) also mentioned that the use of BAC may quantify the exposure to a metal(loid) more accurately than other methods. Moreover, whereas it is typically assumed that 100% of the As present in the dust or soil is bioaccessible for the purpose of health risk assessment, this assumption may be an overestimation. In this context, the partial dissolution of a component from particulate matter and soil has been reported in various studies (Gray *et al.*, 2010; Niu *et al.*, 2010; Caboche *et al.*, 2011; Drysdale *et al.*, 2012; Boisa *et al.*, 2014; Wiseman and Zereini, 2014). Particularly in areas affected by gold mining activities, increasing numbers of studies have been conducted to determine the bioaccessible fraction of As (Meunier *et al.*, 2010; Ono *et al.*, 2012; Toujaguez *et al.*, 2013; Ng *et al.*, 2014; Ono *et al.*, 2016; Drahota *et al.*, 2018; Martin *et al.*, 2018). These studies have indicated that the BAC of arsenic is mostly dependent on the mineralogy of the samples.

Mineral Liberation Analyzer (MLA) constitutes a scanning electron microscopy (SEM)-based automated image analysis system (Gu, 2003; Fandrich *et al.*, 2007). MLA was originally developed for metallurgical and geological samples and subsequently adapted to the analysis of atmospheric dust by our group (Gasparon *et al.*, 2016; Elmes and Gasparon, 2017; Ciminelli *et al.*, 2018). We further demonstrated that the technique is suitable to quantitatively analyze both crystalline and non-crystalline phases in environmental samples, and to provide statistically-sound, single particle data on the particle size, morphology, elemental composition, and mineralogy of soil samples (Ciminelli *et al.*, 2018).

Paracatu, a city located in the Brazilian state of Minas Gerais, is influenced by mining activities due to its proximity to a gold mine. It is a typical historic township established during the 18th century following the discovery of gold. Despite the current best practice technology and stringent environmental control, communities situated in mineral-rich regions may be exposed to elevated concentrations of potentially harmful elements, such as As, derived either from the natural rocks, soils, and water, or from mine wastes accumulated over centuries of mining activities. The potential exposure through windborne dust and consequently the effects of As in lung has been a matter of concern in communities living close to historical and current mines (Martin *et al.*, 2018). Therefore, As exposure through air may currently constitute a major concern among the local population and regional authorities.

The purpose of this study was to generate data for the assessment of surface dust (particle size  $\leq 250 \mu\text{m}$ ) and fine surface dust (FSD, fraction  $\leq 10 \mu\text{m}$ ) contributions to total As exposure in Paracatu, Brazil and to identify the sources and distribution of As in samples collected in residential and operational areas of a local gold mine company. To address this issue, a novel approach to analyze FSD is presented. The approach was built on previous works of our group (Gasparon *et al.*, 2016; Elmes and Gasparon, 2017; Ciminelli *et al.*, 2018). Within this context, samples of surface dust were collected in Paracatu township residential areas in close proximity to the gold mine and analyzed for BAC. The bioaccessible As concentration was used to estimate the daily total As intake from unintentional surface dust ingestion and FSD inhalation for adults.

To investigate the bioaccessible As of FSD and its sources, the mineral phases and other components present in selected samples were identified and quantified using MLA. To the best of the authors' knowledge, the MLA technique is used for the first time in this study to analyze FSD. In addition, scanning transmission electron microscopy (STEM) techniques were employed to provide thorough characterization of the finest particles down to 100 nm size. The combination of ingestion and inhalation BAC and statistically robust mineralogical data represents an important advance in the assessment of potential toxicity of As-bearing particles.

## 2 LITERATURE REVIEW

### 2.1 Arsenic in Gold Mining Areas

Arsenic is a naturally occurring element that is widely distributed in trace amounts in the Earth's crust. The concentration of arsenic in soil varies widely, generally ranging from about 1 to 40mg/kg (parts per million - ppm) with an average level of 3–4mg/kg (ppm). In case of soils located in the vicinity of arsenic-rich geological deposits or agricultural areas where arsenic pesticides had been applied in the past may contain higher levels of arsenic. Some arsenic compounds have been produced and used commercially for centuries. Current and historical uses of arsenic generally include pharmaceuticals, wood preservatives, agricultural chemicals, and semiconductor industries. This element was also used in some medicinal applications until the 1970s (ATSDR, 2007).

If an individual swallows levels of inorganic arsenic ranging from about 0.3 to 30mg/L (ppm) in water, he/she may experience irritation of stomach and intestines, with symptoms such as stomachache, nausea, vomiting, and diarrhea. Perhaps the single-most characteristic effect of long-term oral exposure to inorganic arsenic is a pattern of skin changes. These include patches of darkened skin and the appearance of small "corns" or "warts" on the palms, soles, and torso, and are often associated with changes in the blood vessels of the skin. Skin cancer may also be developed. Swallowing arsenic has also been reported to increase the risk of cancer in the liver, bladder, and lungs. Similarly, animal data identify effects on the respiratory system as the primary noncancer effect of inhaled inorganic arsenic compounds, although only a few studies are available (ATSDR, 2007).

Sources of arsenic to air include use and resuspension of arsenic-based pesticides, mining, smelting, manufacturing and waste-disposal activities (Brotons *et al.*, 2010). Arsenic may be introduced into the atmosphere directly from these processes, or it may be derived from sediment and soil particles being entrained into the atmosphere (IARC, 2004). Other important source of arsenic are residues from fossil fuel combustion and particulates generated by forest fires.



The time course of arsenic excretion in humans exposed by inhalation has not been thoroughly investigated, but urinary arsenic levels in smelter's workers rose within hours after they came to work on Monday and then fell over the weekend (Vahter, 1986). This implies that excretion is fairly rapid. This conclusion is supported by intratracheal studies in rats (Rhoads and Sanders 1985) and hamsters (Marafante and Vahter 1987).

Gold mine industries normally deal with arsenic in their deposits, once the metal is associated with arsenic minerals in most cases. These arsenic minerals are a good tracer to identify the presence of gold. For this reason, the chemistry of arsenic in the various environmental compartments as well as its toxicity to humans and biota need to be well understood by the gold mining industries.

Arsenic occurs in two main classes of minerals in this environment: sulfides and oxides (Keshavarzi *et al.*, 2012). Therefore, it can form sulfide minerals such as orpiment ( $\text{As}_2\text{S}_3$ ), realgar ( $\text{As}_2\text{S}_2$ ) and arsenopyrite ( $\text{FeAsS}$ ). The latter is the predominant arsenic mineral in the area of the present study.

Arsenic-bearing sulfide minerals occur in sediments, soils, and in a variety of mineralized rocks. Most sulfide minerals are very stable and insoluble in water if they are left undisturbed under anaerobic conditions in the subsurface. However, sulfide minerals may decompose if natural processes or mining and other human activities bring them into contact with water and oxygen. Once oxidized, sulfide minerals may release potentially toxic sulfuric acid and soluble trace elements such as arsenic. This process, called *acid rock drainage*, will not be discussed on this study as it refers only to a potential impact in water not in particulate matter or FSD, focus of this investigation.

Rezende *et al.* (2015) determined the concentration of arsenic in sediments in the area of this study aiming to evaluate the arsenic distribution, mobility and transport in this environment compartment. In this case, some high levels for arsenic were found (up to 2,750mg/kg), however the results demonstrated low mobility to the water course and even to plants, mainly because Fe and Mn oxyhydroxides and Al minerals are present, which significantly immobilizes As in the solid phases. Ono *et al.* (2012) had similar conclusion

when assessing the mobility of arsenic in soils in the same region using a solution similar to human gastrointestinal fluid in order to assess the amount of arsenic that would be absorbed by the gastrointestinal tract in case of accidental ingestion of soils. The reason for this low arsenic mobility can be attributed to the soil's mineralogy in the area of study.

## **2.2 Air Pollution and Particulate Matter**

Air pollution has been an ever-increasing environmental challenge facing both industrialized and developing nations due to its coverage and impacts. As a consequence, this problem is getting the global attention of the policymakers (Basha *et al.*, 2010), and the scientific community. According to Kelly and Fussell (2012), urban air pollution is a major contributor to the worldwide human disease burden ranging from respiratory complications to cancer. In fact, it has been recognized as carcinogenic to humans, with the International Agency for Research on Cancer (IARC) concluding that there is sufficient evidence to attest the carcinogenicity of outdoor air pollution (IARC, 2013).

A major component of air pollution that has also been classified by the IARC as a human carcinogen is particulate matter, which is considered a key parameter in air quality monitoring due to its negative impacts on human health, environment, and atmospheric chemistry (IARC, 2013). Particulate matter (PM) can affect the ecosystem and human health, particularly when particles are loaded with potentially toxic elements and compounds (Basha *et al.*, 2010). Concomitantly, dust is a major pathway for the transport and redistribution of environmental pollutants from point sources, such as active mine sites, or larger distributed sources like urban conglomerations and industrial centers. Re-suspended road dust emissions were found to be the dominant mechanisms that contribute significantly to the total PM<sub>10</sub> and PM<sub>2.5</sub> emission factors (Abu-Allaban, 2003) and these particle sizes may contribute up to 30% to total urban PM.

“Heavy metals”, the term that is commonly applied to toxic elements, are a primary concern in mining operations due to geological enrichments of certain elements, metals or not, in the local mineralization, which defines the mine site. As such, the huge potential of mine sites to be point sources of pollutants in water, soil, and air requires a full

understanding of all relevant contaminant transport pathways in order to manage the prospective impacts. Amongst the possible pathways for elemental contaminant transport (soil, groundwater, surface water, biota, and air), particles in the atmosphere should be notable due to faster vector velocity, and greater aerial extent of redistribution (Csavina *et al.*, 2012). And despite the notable risks to human health, relatively little is known about the heterogeneous chemistry, and latent reactivity of airborne dust particles in areas under the influence of mining operations. Specific to the minerals industry, a holistic approach should be conducted to assess dust from mining operations. This should include studies on source apportionment, understanding variations between size fractions and multiple forms of analyses for minimal bias in sampling methods. In addition, it should involve well-accepted procedures to evaluate the toxicity of a target air particulate to the nearby communities.

### **2.3 Bioavailability and Bioaccessibility**

Metal(loid) concentrations are recognized as a useful index of air pollution (Shaheen *et al.*, 2005). As such, several studies have been carried out to characterize the elemental composition of dust and soil because of the toxic nature of certain trace elements (Zheng *et al.*, 2013; Huang *et al.*, 2014b; Wiseman and Zereini, 2014; Drahota *et al.*, 2018; Ciminelli *et al.*, 2018).

Decisions on the selection of sites that require remediation are made following site investigations and the application of a risk characterization procedure. Most regulations and accepted regulatory assessment procedures are still based on total concentrations of contaminants and do not take into account the likelihood that contaminants will become available in forms that may adversely impact human health or the environment (Harmsen and Naidu, 2013). Although in water the dissolved contaminants are readily available to be absorbed, in soils or dusts the element of interest may be found in different compounds with various forms of association with the other constituents in the solid matrices. Therefore, various investigations related to soils and dust can lead to an unrealistic assumption that 100% of the contaminant is available to be absorbed by the organism into a systemic circulation and potentially cause an adverse effect to health. So, some

approaches are needed to avoid the overestimation of the risk. Remediation programs can take longer time to be implemented and costs increase in case of risk overestimation. In this context, two specific tools have been frequently used by the scientific community. They are the bioavailability and bioaccessibility tests, which are commonly called by *in vivo* and *in vitro* tests, respectively.

Ruby *et al.* (1999), defined bioavailability (BA) as the fraction of an element that reaches circulatory system compartment from the gastrointestinal tract. It can be defined as “absolute bioavailability”, and is equal to the oral absorption fraction. Relative bioavailability is the comparative bioavailability considering the same element in different media (e.g. water, soil, food). For instance, the relative bioavailability of a contaminant is the ratio between the absolute bioavailability of this contaminant in soil and the absolute bioavailability of the same contaminant in water.

Bioavailability has been developed to predict the human exposure to a specific element of interest and uses animals to determine the amount of an element bioavailable in the blood. The choice of animal to be tested to estimate the bioavailability of an element in humans requires a selection based on the similarity of age, anatomical and physiological characteristics. Therefore, in these studies, pigs are preferred by the similarity to humans of the digestive tract, nutritional needs and mineral metabolism. Vodička *et al.* (2005) claim that the miniature pig not only share many physiological similarities with humans but also offers several breeding and handling advantages (when compared to non-human primates), such as lifetime, gestation period, easiness to maintain in controlled conditions, making it an optimal species for preclinical experimentation.

The tests *in vivo* are expensive, time consuming, require specialized personnel in the treatment of animals and require appropriate infrastructure to be run (Hettiarachchi and Pierzynski, 2004). These tests raise many debates from NGO's responsible for protecting the animals, once the animals are put into extremely hard conditions. In this context, an alternative suggested by Ruby *et al.* (1993) is the bioaccessibility (BAC) test, which is performed in laboratory with solutions that simulate the physicochemical conditions of the human body.

In the last decades, bioaccessibility methods have been widely adopted for the estimation of bioavailability for risk assessment of metal-contaminated sites to avoid the high costs and ethical considerations associated with tests carried out with animals (Diacomanolis *et al.*, 2007; Guney *et al.*, 2017).

Bioaccessibility tests are often related to the solubility of metals from mineralized rock or waste material in general. For instance, Ruby *et al.* (1999) states that bioaccessibility and bioavailability studies suggest that arsenic present in sulfide minerals such as arsenopyrite has a low relative bioavailability when compared to iron/manganese-arsenic oxides, for a constant particle size. Therefore, the mineralogy of the material is one of the most important information to evaluate an element's dissolution. This information has to be considered in environmental or health risk assessment in mining areas, which are naturally abundant in a variety of minerals. In addition, the bioaccessible fraction of an element is a relevant information for communities that live nearby these operations, NGO's and regulators. Finally, this information could bring a more realistic plan for remediation programs, when necessary and a more technical approach for regulators.

## **2.4 Bioaccessibility in gastrointestinal media**

Soil unintentional ingestion can be an important exposure route for a specific metal(loid). Therefore, the use of methodologies to understand the amount of an element that is really available for the humans through the gastrointestinal pathway is important and allows a more realistic health risk assessment.

Oral bioaccessibility is regularly used to investigate the amount of a contaminant that can be absorbed by the gastric and intestinal systems and may reach to the blood. The first step is the total or partial release of the contaminant in a solution that mimics the digestive juice chime (gastric phase), which has a more acidic environment. These contaminants can subsequently be extracted by intestine, which has relatively high pH values (neutral). In this phase, a more favorable contaminant absorption happens when comparing to

gastric phase, although the latter can extract higher amount of the contaminant due to acid conditions.

There are several methods to determinate the oral bioaccessibility of an element and they can present different results depending on the selected gastric pH and solution composition. The main methods are described below.

The physiologically based extraction test (PBET) and the simple bioaccessibility extraction test (SBET) have been successfully used to estimate the oral bioaccessibility of soil metals. The PBET protocol comprises the extraction in gastric and intestinal fluids. SBET is a simplified form of PBET and therefore is a faster, easier extraction test (Gu *et al.*, 2016). It simulates only the gastric phase in acid condition, not employing the intestinal compartment (Oomen *et al.*, 2002). PBET has been widely adopted for the estimation of bioavailability (Diacomanolis *et al.*, 2007; Juhasz *et al.*, 2007; 2009a; 2009b) and offers a potentially superior approach for *in vitro* methods (Kim *et al.*, 2001). In addition, the IGV bioaccessibility test, which consists in determining the level of a contaminant in two phases (gastric and intestinal) was chosen for this kind of study.

Bioaccessibility tests of arsenic and other elements have been validated against in-vivo models. The use of bioaccessible concentrations in health risk assessment is accepted by the United States Protection Agency (USEPA) and is recommended as part of the National Environmental Protection Measure (NEPM) review (Ng *et al.*, 2010).

Size fraction for oral bioaccessibility is a key parameter to develop health risk assessment. The  $\leq 250 \mu\text{m}$  fraction is regarded as the particle size fraction that is likely to adhere to fingers and hence could result in exposure via hand-to-mouth (Duggan *et al.*, 1985; Drahota *et al.*, 2018).

A review of the various methods applied to determine the bioaccessibility is presented by Oomen *et al.* (2002) and is beyond the scope of the present investigation. The present study adopted the PBET method to assess the As oral bioaccessibility of samples collected in residential areas.

## 2.5 Bioaccessibility of Arsenic in Simulated Lung Fluids (SLF)

Bioaccessibility in simulated lung fluids follows similar principles of bioaccessibility for gastrointestinal tract. It is an *in vitro* test that determines the percentage of an element that is soluble in a solution similar to the human lung extracellular liquid. Therefore, by this test, it is possible to evaluate the health risks associated with the inhalation pathway of exposure to an element of interest.

Soluble phases associated with particulate matter have been identified as being of main concern, due to their predicted higher bioavailability and, in turn, likely greater toxic potential (Wiseman, 2015). Compared to their insoluble counterparts, soluble metals are generally more likely to quickly enter into systemic circulation and be translocated to other organs such as the heart upon uptake in the lung (Wallenborn *et al.*, 2007).

There are several approaches to simulate a synthetic lung fluid (Caboche *et al.*, 2011; Boisa *et al.*, 2014; Wiseman, 2015). The most common are water, the Artificial Lysosomal Fluid (ALF) and Gamble's solutions, which are explained below. Therefore, it would be reasonable to assume that the choice of leaching solution could interfere in the outcome and results of a bioaccessibility study. In that sense, comparisons among results obtained in different studies need to have a degree of caution (Martin *et al.*, 2018).

The use of pure water is widely reported in the literature and this can be justified by analytical constraints generated by using complex solutions to mimic the human lung. Furthermore, this media is far less expensive and complex than others, which require a gamma of analytical reagents. Nevertheless, the bioaccessible fraction of an element in lung cannot be accurately accessed by its dissolution in water. Caboche *et al.* (2011) compared the extraction rate of four airborne standard reference material (SRM) using pure water and Gamble's solution and the conclusion was that, although water has a slight lower pH (7 against 7.4), it does not extract metals with the same efficiency. In that study, the bioaccessibility calculated for water was smaller than that from the Gamble's solution, mainly due to the difference in the solution chemistry, which will be discussed further. This finding demonstrates that simulated lung fluid can dissolve more compounds than

ultra-pure water, so that the use of water underestimates the pulmonary bioaccessibility of metals compounds.

The Artificial Lysosomal Fluid (ALF) is expected to simulate the intercellular conditions in lung cells occurring in conjunction with phagocytosis, therefore representing relatively harsh, untypical conditions. It can also represent the cellular conditions that exist following an immune response in the lung (Caboche *et al.*, 2011; Wiseman and Zereini, 2014). As ALF tries to simulate an immune response, the pH is more acidic (4.5). Table 2.1 shows the chemical composition of ALF.

The most common extractor is the Gamble's solution or its modified methods. It can be considered as the pioneer synthetic lung fluid and has been widely used for the exposure assessment of humans to inhalable pollutants (Boisa *et al.*, 2014). Gamble (1941) described the physiological fluids and his work served as a basis for a number of experimental proposals using solutions to mimic the human intercellular fluid (Jurinski and Rimstidt, 2001). Gamble's solution is a mixture of inorganic salts, carbonates, chlorides and various metal phosphates in a neutral pH (Wiseman *et al.*, 2015) considered to be virtually identical to the lung fluid in terms of major components (Davies and Feddah, 2003). It was first developed for determining *in vitro* toxicity of radioactive compounds (Caboche *et al.*, 2011) and passed through modifications over the years to adapt to the objectives of different investigations. Table 2.2 summarizes solution compositions reported in the literature. Almost all methods are similar when comparing the inorganic salts to generate the lung fluid.

Wiseman (2015) observed that there are important variations in the composition of the synthetic lung fluid used to mimic the dissolution of metals following inhalation, and no standard method is available for conducting metal extraction. This is due, in part, to the difficulties associated with simulating the complex lung conditions *in vitro*. The Simulated Epithelial Lung Fluid (SELF), for instance, brings additional proteins (e.g. albumin, mucin, and uric acid) compared to the Gamble's solution (Boisa *et al.*, 2014). Some authors substituted these proteins with citrate/citric acid (Gray *et al.* 2010; Caboche *et al.*, 2011). This is the approach selected for the present investigation.



Table 2.1: Chemical composition of ALF (pH 4.5) (Wiseman, 2015)

<b>Chemical constituents</b>	<b>Amount (g/L)</b>
Magnesium chloride (MgCl <sub>2</sub> )	0.050
Sodium chloride (NaCl)	3.210
Calcium chloride (CaCl <sub>2</sub> )	0.128
Sodium sulfate	0.039
Disodium hydrogen phosphate (Na <sub>2</sub> HPO <sub>4</sub> )	0.071
Sodium citrate dehydrate (NaH <sub>2</sub> C <sub>6</sub> H <sub>5</sub> O <sub>7</sub> ·2H <sub>2</sub> O)	0.077
Sodium hydroxide (NaOH)	6.000
Citric acid (C <sub>6</sub> H <sub>8</sub> O <sub>7</sub> )	20.800
Glycine (NH <sub>2</sub> CH <sub>2</sub> COOH)	0.059
Sodium tartrate dehydrate (C <sub>4</sub> H <sub>4</sub> O <sub>6</sub> Na <sub>2</sub> ·2H <sub>2</sub> O)	0.090
Sodium lactate (C <sub>3</sub> H <sub>5</sub> NaO <sub>3</sub> )	0.085
Sodium pyruvate (C <sub>3</sub> H <sub>3</sub> O <sub>3</sub> Na)	0.086

Table 2.2: Chemical composition of Gamble's solutions (pH 7.4) (Boisa *et al.*, 2014)

Composition (mg/L)	Original Gamble solution	Pseudo alveolar fluid	Simulated lung fluid	Artificial interstitial fluid	Gamble solution*	Modified Gamble solution	Synthetic serum	Gamble solution*	Simulated epithelial lung fluid
MgCl <sub>2</sub> ·6H <sub>2</sub> O	203	212	212	203					200
NH <sub>4</sub> Cl					535	5,300	535	118	
NaCl	6,019	6,415	6,400	6,193	6,786	6,800	6,786	6,400	6,020
CaCl <sub>2</sub>					22		22		
CaCl <sub>2</sub> ·2H <sub>2</sub> O	368	255	255	368		290		225	256
Na <sub>2</sub> SO <sub>4</sub>	71	79		71					72
H <sub>2</sub> SO <sub>4</sub>					45	510	45		
Na <sub>2</sub> SO <sub>4</sub> ·10H <sub>2</sub> O			179						
Na <sub>2</sub> HPO <sub>4</sub>		148	148	142				150	150
NaH <sub>2</sub> PO <sub>4</sub>	142				144		144		
NaH <sub>2</sub> PO <sub>4</sub> ·2H <sub>2</sub> O						1,700			
H <sub>3</sub> PO <sub>4</sub>						1,200			
NaHCO <sub>3</sub>	2,604	2,703	2,700	2,604	2,268	2,300	2,268	2,700	2,700
Na <sub>2</sub> CO <sub>3</sub>						630			
NaHC <sub>4</sub> H <sub>4</sub> O <sub>6</sub> ·2H <sub>2</sub> O (sodium hydrogen tartrate dihydrate)		180	180						
H <sub>2</sub> C <sub>6</sub> H <sub>5</sub> O <sub>7</sub> Na·2H <sub>2</sub> O (sodium hydrogen citrate dihydrate)	97	153	153						
CH <sub>3</sub> CHOHCOONa (sodium citrate)		175			52		52	160	
Citric acid·H <sub>2</sub> O						420			
NaOCOCOCH <sub>3</sub> (sodium pyruvate)		172	172						
NH <sub>2</sub> CH <sub>2</sub> COOH (glycine) (Gly)		118	118		375	450	450	190	376
L-Cysteine (C <sub>3</sub> H <sub>2</sub> NO <sub>2</sub> S)					121				122
DPPC (dipalmitoyl phosphatidyl choline) (C <sub>40</sub> H <sub>80</sub> NO <sub>8</sub> P)								200	100
CH <sub>3</sub> COONa·3H <sub>2</sub> O (sodium acetate trihydrate)	953			952					
Sodium acetate (CH <sub>3</sub> COONa)						580			
HOC (COONa) (CH <sub>2</sub> COONa) <sub>2</sub> ·2H <sub>2</sub> O (sodium citrate dihydrate)				97		590			
C <sub>3</sub> H <sub>5</sub> NaO <sub>3</sub> (sodium lactate)			290						
KCl	298			298					298
Potassium hydrogen phthalate (C <sub>8</sub> H <sub>5</sub> KO <sub>4</sub> )						200			
C <sub>14</sub> H <sub>23</sub> N <sub>3</sub> O <sub>10</sub> (DTPA) (pentetic acid)					79				
C <sub>21</sub> H <sub>38</sub> NCl(ABDAC)					50				
Ascorbic acid									18
Uric acid									16
Glutathione									30
Albumin									260
Mucin									500
pH (adjustment with HCl)		7.6		7.4	7.3	7.4	7.3		7.4

\*Different authors

Some key parameters affecting extraction, such as pH and temperature, are not well established and may vary widely. The ALF, for instance, has lower pH than Gamble solution or pure water and this may affect the extraction rate of a substance. In addition, few studies extracted samples at room temperature instead of 37°C, which has been emphasized as being an essential part of a best practice approach to dissolution testing in pharmaceutical science.

The time selected for extraction is also an important parameter affecting the levels of bioaccessible fractions. Experiments reported by Caboche *et al.* (2011) demonstrated that in a range of 15 to 4,320 minutes (72 h), the equilibrium for dissolution of metals is attained within 24 and 48 hours. Thus, it appears that an extraction-time within this range is adequate to estimate the upper limit of metals bioaccessibility. Nevertheless, the equilibrium time should be confirmed in each case as it will depend on the nature of As-bearing compounds. Martin *et al.* (2018) reported a fast dissolution of arsenic in the first 8 hours of test. In this case, 75 to 82% of arsenic bioaccessible was released within the first 8 hours. The solid liquid ratio (S/L) can also interfere with the extraction time. For instance, a high solid load can lead to longer time requirements. In addition, in high S/L ratios solution can reach saturation, with consequent precipitation, thus leading to underestimation of bioaccessibility (Caboche *et al.*, 2011; Wiseman, 2015).

Dissolution of a target component from particulate matter has been broadly investigated (Gray *et al.*, 2010; Niu *et al.*, 2010; Caboche *et al.*, 2011; Drysdale *et al.*, 2012; Boisa *et al.*, 2014; Wiseman and Zereini, 2014). Particularly in areas affected by gold mining activities, increasing numbers of studies have been conducted to determine the bioaccessible fraction of As (Meunier *et al.*, 2010; Ono *et al.*, 2012; Toujaguez *et al.*, 2013; Ng *et al.*, 2014, Ono *et al.*, 2016), but just few assessed As in a SLF (Drahota *et al.*, 2018; Martin *et al.*, 2018).

Niu *et al.* (2010) studied the solubility of trace elements other than arsenic in different sizes of urban airborne particulate matter in Ottawa for nano (57 to 100nm), fine (100 to 1,000nm) and coarse particles (1,000 to 10,000nm) showing the influence of the chemical composition related to particulate size. The authors observed a general increasing trend

in bioaccessibility with the decrease of particle size and also concluded that the main sources for nano and fine particles are vehicular combustion and emission. Wiseman and Zereini (2014) assessed the metal(loid) solubility (including arsenic) in airborne particulate matter (PM<sub>10</sub>, PM<sub>2.5</sub> and PM<sub>1</sub>) through two different extractors (Gamble's solution and artificial lysosomal fluid - ALF) in Frankfurt – Germany and concluded that the solubility of arsenic was high in both cases. In ALF, the bioaccessibility of arsenic was 89%, 81% and 82% for PM<sub>10</sub>, PM<sub>2.5</sub> and PM<sub>1</sub> respectively, while in Gamble's solution the bioaccessibility was 57%, 64% and 80% for the same particles size. The authors explained that solubility is strongly pH dependent and this is the reason for the difference in bioaccessibility values for both methods. This study also indicated that the total levels of arsenic present in the samples were relatively low compared to the other elements. Consequently, the exposure was low, regardless the high solubility. Hu *et al.* (2012) also studied the bioaccessibility of arsenic and heavy metals for particulate matter with different particle sizes (total suspended particulates – TSP and PM<sub>2.5</sub>) by using a simulated gastric solution for arsenic extraction (SBET – Simplified Bioaccessibility Extraction Test). As this solution tends to mimic the gastric phase, this study might not demonstrate the behavior of the arsenic in the human lung. Although the bioaccessibility of arsenic and other metals were considered high in this study (for arsenic the bioaccessibility was 47.5% and 48.2% for TSP and PM<sub>2.5</sub> respectively), the carcinogenic risk through the inhalation exposure was within the acceptable level. Heal *et al.* (2005) studied the dissolution of arsenic and other metals in PM<sub>10</sub>, PM<sub>2.5</sub> and black smoke in Edinburgh – UK by applying pure water at room temperature followed by hot concentrated HNO<sub>3</sub>/HCl as the extractor agents. Water was chosen due to the simplest and most universal extraction procedure that would not influence metal determination. Results demonstrated that the main sources for trace metals in PM<sub>10</sub> and PM<sub>2.5</sub> were traffic and crustal dust, as the metals more associated with traffic (Cu, Fe, Mn, Pb, Zn) were found to show stronger correlation with suspension/resuspension of vehicle wear or crustal dust than direct exhaust emission. Different correlation was found for arsenic and other metals, which showed stronger correlation with black smoke, which is associated with direct combustion. Solubility of arsenic in water was close to 60% for PM<sub>10</sub> and PM<sub>2.5</sub> in this study.

Huang *et al.* (2014a) and Huang *et al.* (2014b) discussed bioaccessibility of arsenic in depth. The authors investigated the solubility of arsenic fraction in PM<sub>2.5</sub> dust, road dust, and household air conditioning (AC) filter dust using a lung simulated serum solution (for household PM<sub>2.5</sub>) and PBET (for road dust and household AC filter). They also determined arsenic speciation in samples collected in Guangzhou - China. The former study revealed that arsenic (V) was predominant in the samples, though the reduction for arsenic (III) occurred during the *in vitro* test using simulated serum solution. This reduction was explained by the use of cysteine in the simulated lung fluid, which is used as the usual pre-reductant to reduce arsenic (V) to arsenic (III) aiming to generate arsine. For the PBET test, the As (V) predominated in the gastric phase rather than in the intestinal phase, which presented relative higher amount of As (III). According to the authors, this reduction may be occurring due to the presence of organic acids and the neutral pH of intestinal phase. As arsenic mobility and speciation are dependent on redox potential (Eh) and pH, As (III) might be retained in more alkaline and reducing environment. These hypotheses need to be further assessed. The second study concluded that the bioaccessibility of arsenic was 29.88%, however no information was provided to explain the reasons for this value. Arsenic was considered to be the most harmful element in terms of non-carcinogenic risks for PM<sub>2.5</sub>, different than for carcinogenic risk, when other element (Cr) presented the most risk results. Carcinogenic and non-carcinogenic risks will be detailed in the next section.

Drahota *et al.* (2018), investigated the lung and oral bioaccessibility of metal(loid) in gold mine wastes, urban soil and road dust in Czech Republic. Arsenic was considered to be most important contaminant with concentrations of 1.15wt%, 2,900mg/kg and 440mg/kg, respectively in each environment. Different particle sizes and extract solutions were selected for lung and oral BAC, respectively (<11 µm and <250 µm – particle size; Gamble's solution and bioaccessibility research consortium method (SBRC) extraction solution). Bioaccessible As in lung and gastric solution ranged from 5.3 (mine waste) to 5.9% (urban soil) and 5.1 (mine waste) to 8.2% (urban soil) respectively. Low BAC values were attributed to sample mineralogy (oral test) and the presence of Fe oxyhydroxides (lung test). Martin *et al.* (2018) investigated the lung BAC of mine wastes using particle sizes lower than 20µm after sieving. Low values of As BAC, determined

by SLF and ranged from 0.020 to 0.036%, were ascribed to the presence of insoluble As-bearing phase in mine waste samples.

As highlighted by several studies, there are some key parameters that interfere in the results of a bioaccessibility test (e.g., type of solution, pH, temperature, S/L, time, particle size), however, the pH is the most important one. Hence, in most cases, the ALF will drive higher BAC values when comparing to the Gamble's solution, which has a more neutral pH.

## 2.6 Human Health Risk Assessment

Human health risk assessment is the procedure to estimate the nature and the probability of a chemical element cause an adverse effect in humans, who may be in contact or exposed to this specific element (USEPA, 2016).

Risk assessment protocols involves two categories, which applies to carcinogenic or non-carcinogenic substances, according to Environmental Protection Agency guidelines. Parameters such as chemical daily intake (CDI), reference doses (RFD) and slope factor (SF) are considered to be important to determine the risk assessment of a metal(loid) (Huang *et al.*, 2014b). Reference dose and slope factor are parameters already defined by the USEPA (Gu *et al.*, 2016) and therefore are not calculated.

USEPA (2019) establishes that daily intake is the amount of a chemical a person is exposed to on a daily basis over an extend period of time. Reference dose is a daily oral exposure to the human population that is likely to be without an appreciable risk of deleterious effects during a lifetime. Slope factor is an upper bound, approximating a 95% confidence limit, on the increased cancer risk from a lifetime exposure to an agent.

Carcinogenic Risk (CR) is the probability of a person to develop cancer, over a lifetime exposure to carcinogenic hazards. It depends on the chemical daily intake (CDI), the bioaccessibility (BAC), which is the ratio of metals' concentrations extracted using a fluid to their total concentrations in a matrix of study (dust, soil). It also depends on the cancer

slope factor (CSF). The linear dose relationship for CSF following guidelines established by USEPA (1995) reported the risk of  $1 \times 10^{-6}$ ,  $1 \times 10^{-5}$ ,  $1 \times 10^{-4}$  as the probability of one additional case of cancer in an exposed population of 1,000,000, 100,000, and 10,000, respectively. The acceptable risk for CR and regulatory purposes ranges from  $1 \times 10^{-6}$  to  $1 \times 10^{-4}$  (Gu *et al.*, 2016; Li *et al.*, 2014). In Brazil, the tolerable risk for carcinogenic substances is one additional case of cancer in a population of 100,000 individuals ( $1 \times 10^{-5}$ ) (BRAZIL, 2009).

Non-carcinogenic risk typically depends on hazard quotient (HQ) (Li *et al.*, 2014). If this value is  $<1$ , there is no significant risk of non-carcinogenic effects. If HQ is  $>1$ , there is a probability that non-carcinogenic risk may occur. Hazardous quotient is the ratio between CDI and RFD.

Other method to determine the health risk assessment is provided by the Joint FAO/WHO Expert Committee on Food Additives (JCEFA, 2011) and considers the Benchmark Dose Lower Confidence Limit (BMDL). It establishes that the inorganic As BMDL for an increase of 0.5% of lung cancer incidence is  $3.0 \mu\text{g}/\text{kg}(\text{b.w})/\text{day}$  (BMDL<sub>0.5</sub>), ranging from 2.0 to  $7.0 \mu\text{g}/\text{kg}(\text{b.w})/\text{day}$  based on epidemiological data.

The BMDL methodology has been more frequently used by health risks assessment studies around the world as there are evidences that the methodology applied by EPA tends to be less appropriate, when considering the provisional guideline value for potable water of  $10 \mu\text{g}/\text{L}$ . Arsenic provisional concentration in drinking water established by WHO (2011) is related to a cancer risk of  $4.29 \times 10^{-4}$ . This value is already slightly in excess of the so-called acceptable risk of  $1 \times 10^{-6}$  to  $1 \times 10^{-4}$  provided by EPA and also higher than the tolerable carcinogenic risk ( $1 \times 10^{-5}$ ) provided by Brazilian regulation. The present study considered the BMDL methodology to evaluate the human health risk assessment of arsenic.

## **2.7 Relevant Brazilian and International Legislation for arsenic in particulate matter**

The Brazilian National criteria and guideline values for soil quality relative to the presence of chemical substances, and the guidelines for environmental management of areas contaminated by these substances as a result of anthropogenic activities are outlined in CONAMA 420 (BRAZIL, 2009). It is noted that this document deals only with soil and groundwater, and does not provide any information on air quality. Neither Brazil nor the World Health Organization have specific guidelines for arsenic in air or FSD, although CONAMA 420 defines as tolerable level of risk to human health, for carcinogenic A1 substances, such as arsenic, the probability of one additional case of cancer in an exposed population of 100,000 individuals. The European Union (EU, 2005) set a “Target Value” of 6ng/m<sup>3</sup> in PM<sub>10</sub>. Considering that ATSDR (2007) mentions that in urban areas the levels of arsenic in the air ranges from 20 to 30ng/m<sup>3</sup>, this target value can be considered very low.

The most comprehensive set of procedures and regulations dealing with the distribution of arsenic in ambient air was published by the European Union in 2005 (EU, 2005). It is important to note that these directives refer to target values, not guideline values, and that the achievement of these target values should: “not require any measures entailing disproportionate costs”. Regarding industrial installations, they would not involve measures beyond the application of best available techniques as required by Council Directive 96/61/EC of 24 September 1996 concerning integrated pollution prevention and control and in particular would not lead to the closure of installations. However, they would require Member States to take all cost-effective abatement measures in the relevant sectors.” (Preamble, Part 5). Further, “target value” is defined as a “concentration in the ambient air fixed with the aim of avoiding, preventing or reducing harmful effects on human health and the environment as a whole, to be attained where possible over a given period.” (Article 2, Definition (a)). The European Union states that target value for arsenic in PM<sub>10</sub> is 6 ng/m<sup>3</sup>, as the average over a calendar year. It also provides specific guidelines on macroscale and microscale sampling point siting, sampling frequency, number of sampling points relative to population, and analytical methods.



In conclusion, although some national and international organizations have developed exposure and total element guidelines, there is no general consensus on which guidelines should apply, and on how threshold values should be calculated (e.g., maximum value, median, mean, and over which period of time). In case of arsenic, no guideline is available to evaluate the level of arsenic that might cause harm to human health by inhalation pathway.

### 3 MATERIALS AND METHODS

#### 3.1 Studied site and sample collection / preparation

The study area is located in a city with approximately 91,000 inhabitants (IBGE, 2015) in the Northwest of Minas Gerais State, Southeast Brazil (Figure 3.1). The main economic activities of the region include agriculture, cattle grazing, charcoal production, and mining. Gold, discovered in the late 18<sup>th</sup> century and usually found in association with geogenic arsenic anomalies, attracted artisanal mining and the early European settlers to this and other regions of Minas Gerais. In the 1980s these activities intensified considerably, resulting in the influx of approximately 5,000 people with the objective of exploiting gold. At the end of this decade these activities were ceased by authorities; however, they had contributed to a significant deterioration of the landscape. Industrial mining has since been in operation. A large gold mine is located immediately to the north of the town of Paracatu, with some residential dwellings situated <1 km from the open pit. The town is located in a typical Brazilian “cerrado” (tropical savanna ecoregion characterized by a rich and unique floral and faunal diversity) and is influenced by a regional tropical system in the mid-latitudes with well-defined dry (April to September) and rainy seasons (October to March).

Surface dust sampling was conducted in seven sites in the residential area of Paracatu (H1 to H7) in two campaigns (dry and wet seasons). These comprised geogenic surface dust samples collected from the ground surface at the proximity of residential areas where citizens may be regularly exposed to re-suspended dust. These samples possibly represent a combination of fugitive dust from construction and excavation sites (including potential material from the mine site), natural geological background, and baseline associated with local and regional industrial and agricultural activities. The collection and storage followed the procedures described in USEPA (1991) and Zheng *et al.* (2010). The ground (top 5–10 mm) was swept with a new and clean polyethylene brush within 1m<sup>2</sup> radius circles around each sampling site, catching the powder with a clean sheet of paper and storing the samples in polyethylene plastic bags, which was accommodated in a closed recipient to avoid the humidity and heat interferences, at ambient temperature for

transportation to the laboratory, where they were completely dried overnight at 40°C in a laboratory oven. Then, the samples were sieved to obtain the  $\leq 250 \mu\text{m}$  particle size fraction, which may easily adhere to fingers (Drahota *et al.*, 2018), in order to simulate the fraction relevant to unintentional soil ingestion through hand-to-mouth activities (Ng *et al.*, 2015), in a procedure consistent with the USEPA (2009). Each sample was stored separately in a plastic bag, which was accommodated in a closed recipient vessel to avoid interference from humidity and heat. The  $\leq 250 \mu\text{m}$  fraction of each surface dust sample was measured for BAC using the Physiologically Based Extraction Test (PBET) (Ruby *et al.*, 1996).

Based on a geographical distribution that comprises a representative sampling network for dust assessment two additional samples of surface dust were collected in the south of the mine during the dry season (H17 and H19) and three samples were selected (H2, H5, and H6) from a total of seven surface dust samples in order to conduct the lung BAC test. In addition, three samples (CP1, CP2, and BP) were collected in the dry season from different crushers areas (CP1 and CP2) and from the gold beneficiation plant (BP). Samples CP1 and CP2 represented dust generated in the operational area and deposited on the surface of equipment and handrails of the area. Sample BP represented the ore after crushing and size classification by cyclone. All samples (excluding BP) were sieved using an ultrasonic assisted shaker (Model VJ-1212, Precision Eforming LLC, Cortland, NY, USA) to obtain the  $\leq 10 \mu\text{m}$  fraction to evaluate the particle size that is likely inhaled by humans (Kastury *et al.*, 2017; Martin *et al.*, 2018). Extracting minor fractions from surface dust in places where citizens are exposed to dust generated from soil was also employed by Drysdale *et al.* (2012), Guney *et al.* (2017) and Drahota *et al.* (2018). FSD was therefore collected on aluminum foil placed at the bottom of a  $10 \mu\text{m}$  stainless steel ring sieve. BP sample ( $\leq 150 \mu\text{m}$ ) was passed through five cyclones (Warman Cyclosizer model M-12, Lahti, Finland) to separate the different sizes of particles. Figure 3.2 presents the area of the study and the sample locations.



Figure 3.1: Northwestern microregion (highlighted in the inset), where the studied site is located, in the state of Minas Gerais, Brazil.

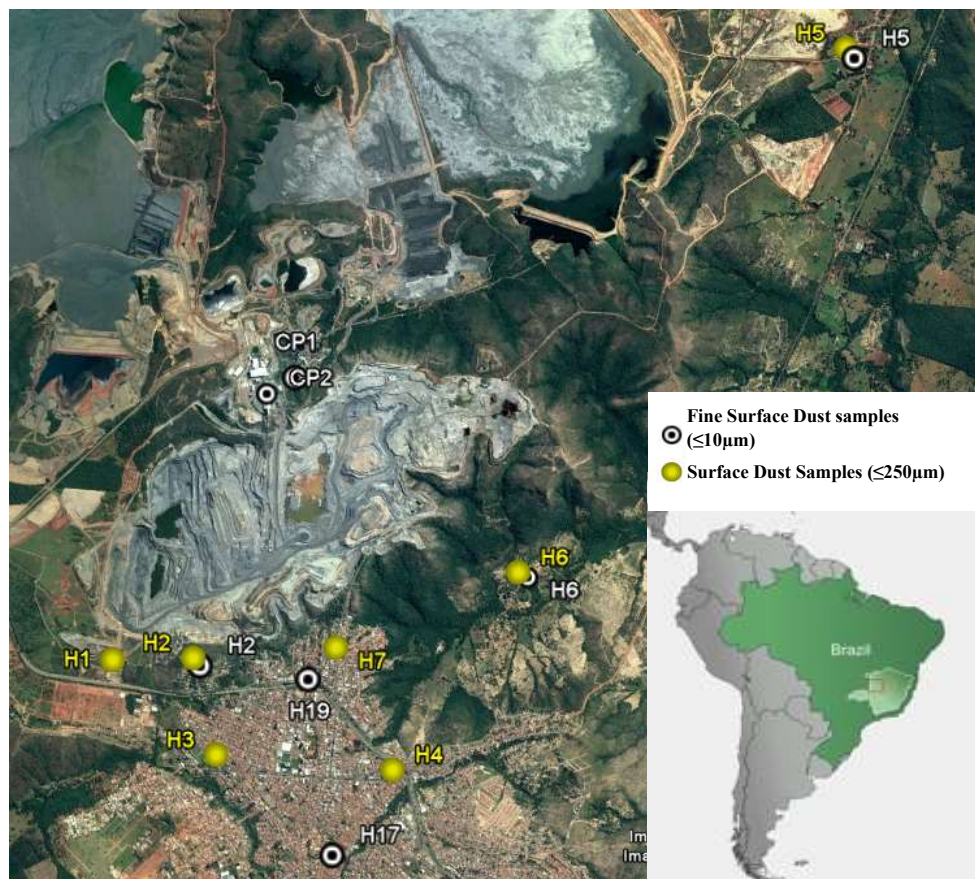


Figure 3.2: Locations where the samples were collected in the town of Paracatu, the state of Minas Gerais, Brazil, and in the industrial site.

## 3.2 Experimental

### 3.2.1 Physiologically based extraction test (PBET)

The BAC of As in surface dust samples was assessed by PBET (Ruby *et al.*, 1996) to simulate the unintentional ingestion of surface dust via the gastrointestinal tract. The  $\leq 250$   $\mu\text{m}$  fraction of each surface dust sample was prepared and added into solutions that simulate the gastric and small intestine phases for 1 and 2 h, following the procedure reported by Zheng *et al* (2013). The analytical procedure was conducted in a water bath (Grant JB Series, Cambridge, UK) at 37°C with oxygen-free conditions created by bubbling argon gas into the solutions. The surface dust sample was extracted using a solid:liquid (S/L) ratio of 1:100. The pH 1.3, 2.5, and 4.0 was adjusted with hydrochloric acid (analytical reagent grade, 10 M) to simulate the gastric phases of a fasting, semi-fed, and fully-fed stomach, respectively, for each surface dust sample (Figure 3.3). Liquid samples were collected after 20, 40, and 60 min for all gastric phase pH conditions generating the total 9 samples. One molar (1M)  $\text{NaH}_2\text{CO}_3$  (1 M) solution was then used to adjust the pH to 7, which simulates the neutral pH condition of the small intestine phase, over a period of 2 h and then 3 more samples were generated. BAC was performed in duplicate unless otherwise specified.

Each extracted solution was filtered through a 0.45  $\mu\text{m}$  membrane filter (Millipore Corporation, Bedford, MA, USA) and diluted suitably with added internal standards prior to the analysis of As using inductively coupled plasma-mass spectrometry (ICP-MS; Agilent 7500cs, Agilent Technologies, Tokyo, Japan). A summary of instrumental parameters is given in Table 3.1. The amount found in each extract was then compared to the actual amount (calculated from the initial total elemental concentration) placed in the gastrointestinal digestion tube to derive the BAC (%) value of As. The overall BAC was taken as the mean of 12 measurements from each of the duplicates to represent the various physiological states of a human during their daily active period.

Table 3.1: ICP-MS (Agilent 7500cs, Agilent Technologies Japan) instrument operational parameters.

<b>Parameters</b>	<b>Conditions</b>
Nebulizer type	Babington Nebulizer
Peristaltic Pump	0.12-0.16rps
Carrier Gas	0.8L/min
Make Up Gas	0.34L/min
Reaction Gas	He at 4.5mL/min



Figure 3.3: Photo of the physiologically based extraction test (PBET) apparatus containing the required enzyme

### 3.2.2 BAC using simulated lung fluid (SLF)

The BAC of As in FSD samples was assessed using an SLF similar to modified Gamble's solution, adapted from Gray *et al.* (2010). The reason for using this leaching agent was to ensure that extraction conditions were biologically consistent with the interstitial fluid in the lung.

For the extractor agent, 500mL of synthetic lung fluid was prepared in a volumetric flask and warmed to 37°C in a water bath (Grant - JB Series, UK) to simulate the temperature of extracellular human lung fluid (Gray *et al.*, 2010; Wiseman and Zereini, 2014). The solution was prepared with NaCl (6,800mg/L), NH<sub>4</sub>Cl (5,300mg/L), NaHCO<sub>3</sub> (2,300mg/L), H<sub>3</sub>PO<sub>4</sub> (1,200mg/L), NaH<sub>2</sub>PO<sub>4</sub>·H<sub>2</sub>O (1,700mg/L), Na<sub>2</sub>CO<sub>3</sub> (630mg/L), Na-acetate (580mg/L), K-acid-phthalate (200mg/L), glycine (450mg/L), H<sub>2</sub>SO<sub>4</sub> (510mg/L), Na<sub>3</sub>-citrate·2H<sub>2</sub>O (590mg/L), CaCl<sub>2</sub>·2H<sub>2</sub>O (290mg/L), and citric acid·H<sub>2</sub>O (420mg/L), which was previously adjusted to pH 7.4 with NaOH. Reagent grade chemicals and Milli-Q (18 MΩ·cm Milli-Q water purification system, Millipore Corporation) water were used in the experiments.

A S/L ratio of 1:20 (w/v) was used for the bioaccessibility test (Table 3.2) by adding 0.1 g of FSD to 2 mL of synthetic lung fluid (37°C) using a 5 mL natural colour plastic tubes. Following this, the vessels were covered with bubble wrap to maintain the temperature constant and placed in an incubator for rotation in a frequency of 33 cycles per minute during 24 hours. This period is adequate to estimate the equilibrium for metal dissolution in simulated lung fluids (Caboche *et al.*, 2011). After 24 hours of extraction in the incubator, the samples were centrifuged for 15 minutes at 2,500 cycles per minute in an Allegra X-15R centrifuge (Beckman Coulter Life Sciences, Lane Cove, NSW, Australia). The supernatant was then filtered through a 0.22 µm filter (Millipore Corporation, Bedford, MA, USA) and 1.5 mL of solution was added to 5 mL plastic vessels filled with 3.5 mL of 2% HNO<sub>3</sub> (Merck Suprapur Nitric Acid 65% w/v, Darmstadt, Germany). Milli-Q water and was used in all procedures. These solutions were stored in the refrigerator and maintained at the temperature of 4°C until ICP-MS analysis.

Table 3.2: Solid Liquid ratio used for bioaccessibility test

	Sample ID	Weight (g)	Simulated Lung Fluid (mL)
Samples	CP1	0.1030	2.0
	CP2	0.1045	2.0
	H2	0.1050	2.0
	H19	0.1058	2.0
	H6	0.1056	2.0
	H5	0.1010	2.0
	H17	0.1060	2.0
QA/QC samples*	Blank 1	0	2.0
	Blank 2	0	2.0
	SRM NIST 2710a	0.1014	2.0
	SRM NIST 2710a	0.1026	2.0
	SRM NIST 2710a	0.1003	2.0
	SRM NIST 2711a	0.1005	2.0
	SRM NIST 2711a	0.1002	2.0
	SRM NIST 2711a	0.1025	2.0

\*Samples analyzed in triplicate

### 3.2.3 Elemental analysis in surface dust and FSD samples

Arsenic concentrations were measured by ICP-MS (Agilent 7500cs, Agilent Technologies, Tokyo, Japan) following an *aqua regia* digestion process in accordance with USEPA 2007. Approximately 1 g of surface dust was accurately weighed into a digestion flask to which 10 mL of *aqua regia* acid mixture was added and allowed to stand overnight at room temperature. The mixture was then placed on a hot plate for the digestion step over 2–2.5 h at 135°C and allowed to cool to room temperature before making up the volume to 100 mL.

For FSD analysis, reverse *aqua regia* was added to approximately 0.05 g of sample (S/L of 1:40) and the solutions were allowed to stand for 3 h before microwave digestion (Milestone Ethos One, Milestone Inc., Shelton, CT, USA). Reverse *aqua regia* was used to minimize the formation of a dimer between the chloride ion (from hydrochloric acid) and the argon gas to form ArCl, as ArCl has the same mass as arsenic (i.e., 75). At high



concentrations, this can interfere with the arsenic signal when using ICP-MS. The temperature was first raised to 110°C, held for 10 min, then to 180°C and held for 40 min. The corresponding power at the two stages was 1400 W. Upon completion, the digested FSD solutions were allowed to cool, diluted to 20 mL, and left overnight before further preparation for ICP-MS analysis. An Allegra X-15R centrifuge (Beckman Coulter Life Sciences, Lane Cove, NSW, Australia) was used to separate the S/L for 15 min at 2500 cycles per minute and 0.5 mL of clear digested solution was transferred to 5 mL plastic tubes containing 4.5 mL of Milli-Q water. Blanks and SRMs were digested in the same manner as part of the QA/QC protocol, however with different quantities.

Ten standards were freshly prepared according to ICP-MS requirement to calibrate the instrument prior to analysis. Internal standard (0.1 mL) was added to each vessel. All samples, standards, blanks, and spikes were analyzed together in ICP-MS. Blanks and Certified Reference Materials (water TM24.3 and sediment BCSS-1), with an optimum sample weight of 0.25 to 0.5 g, were digested in the same manner as part of the quality control protocol during the PBET extraction. The recovery of As was 94.8% and 99.8% for TM24.3 and BCSS-1, respectively. Standard and Certified Reference Materials (NIST 2710a, 2711a, PACS-2, and MESS-3) were used during the extraction of As in FSD samples. The recovery of As was within 85–89% of NIST and 87–88% of PAC and MESS values (Table 3.3).

Table 3.3: Quality control data for arsenic analyses.

<b>Reference Material</b>		<b>As (mg/kg)</b>
Water CRM TM24.3	Measured	4.94
	Certified value	5.21
Sediment CRM BCSS-1	Measured	11.88
	Certified value	11.9±1.4
SRM NIST 2710a	Measured	1373.07±8.35
	Certified value* (range) ***	1540±100 (1300-1600)
SRM NIST 2711a	Measured	91.20±1.72
	Certified value** (range) ***	107±5 (81-112)
CRM PACS 2	Measured	23.18
	Certified value	26.2±1.5
CRM MESS 3	Measured	18.46
	Certified value	21.2±1.1

\*Montana I soil (2009); \*\*Montana II soil (2009); \*\*\*Montana I and II soils (2010).

BP, H2 and H19 samples were analyzed for different parameters. Total sulphur was determined using a combustion furnace (LECO, SC632, USA). Major elements (Al and Si) were measured using an energy-dispersive X-ray fluorescence spectrometer (EDXRF, Shimadzu EDX-7000, Japan). Inductively coupled plasma-optical emission spectrometry (ICP-OES; Perkin Elmer, model Optima 7300DV, USA) (Table 3.4) was used to determine the concentrations of Fe and As, following the acid digestion in *aqua regia* (HNO<sub>3</sub>/HCl - 3:1) (USEPA, 2007). All reagents and experiments were prepared using Milli-Q water (18MΩ.cm Milli-Q water purification system, Millipore Corporation, Bedford, USA). The certified reference materials included the Montana I Soil SRM NIST 2710a (NIST, Washington D.C. USA), the Base Metals Ores CCRMP MP-1b and the CCRMP NBM-1 (NRC, Canada), which were analyzed in the same manner as the samples with an optimum sample weight of 0.1 to 0.2 g. Duplicates and replicates were carried out in each batch. Representative procedure blanks were prepared with standard reference materials (SPEX CertiPrep 1000 mg L<sup>-1</sup>, NJ, USA) and included in each batch run of every 10 samples. All blank extractions returned values below the method detection limits (DL<0.2 mg L<sup>-1</sup>). The standards allow for the evaluation of instrument performance and assay precision. Recoveries ranged from 100 to 110%.

Table 3.4: Instrumental conditions (ICP-OES)

<i>Parameter</i>	<i>Condition</i>
Radiofrequency (W)	1300
Internal Spike	Lu 1 mg/kg
Nebulizer	MiraMist
Nebulizer Ar flow	0.80 L/min
Alumina injector (mm)	2.0
Plasma Ar flow (L/min)	15
Auxiliary Ar gas (L/min)	0.8
Sample flow (mL/min)	1.30
Wash between samples (s)	45
$\lambda$ (nm)	As 193.7 radial; Fe 259.939 radial

### 3.2.4 Microscopy-based mineralogical quantification by Mineral Liberation Analyzer (MLA)

The leaching behavior of solid materials is largely dependent on the mineralogical characteristics of the solid phase (Ettler *et al.*, 2003). In this context, having information about the mineralogy of a solid material is essential to understand its components solubility. Therefore, mineralogical composition can be related to leaching of particular elements (Dung *et al.*, 2015).

MLA was used to identify the FSD and ore main constituents. This method consists of specially developed software package and a standard modern scanning electron microscopy (SEM) fitted with energy disperse spectrum (EDS) analyser. Back scattered electron (BSE) signals emitted from a SEM is used to determine the mineral phases of the sample (Gu, 2003). This method can generate high quality resolution images of particle sections when stable BSE signals from modern SEM are available (Franchich *et*

*al.*, 2007), which basically provides images in gray tones proportional to the signal generated between the interaction of the electron beam and the sample (CETEM, 2004). On these images, the gray tons are proportional to the number of electrons and consequently to the average atomic weight. Therefore, the mineral phases of the sample are linked to each gray tom of the image.

The MLA system comprises a FEI Quanta 650 F field emission gun SEM equipped with two Bruker Quantax X-Flash 5030 EDS detectors and FEI MLA suite 3.1.1.283 for data acquisition and processing. In the present study, the grain-based X-ray mapping measurement mode was applied for identification of materials and a series of BSE images were collected. The grains were selected for X-ray mapping through a BSE trigger (Fandrich *et al.*, 2007). A summary of instrumental parameters is given in Table 3.5.

Table 3.5: SEM and MLA parameters.

SEM Parameters		MLA Parameters	
Voltage (kV)	25	Scan Speed ( $\mu\text{s}/\text{px}$ )	8
Working Distance (mm)	11	Resolution (px)	500 x 500
Probe current (nA)	20	Pixel size ( $\mu\text{m}/\text{px}$ )	0.6
Spot size	5.1	Acq. Time (ms)	12
Brightness	93.77	GXMAP BSE trigger	20 – 255
Contrast	19.40	Minimum grain size (px)	10
BSE Calibration	Au 245	GXMAP X-ray step (px)	6

The samples in MLA studies are generally prepared in the form of polished sections (prepared in epoxy resin), which was performed for the ore sample. This technique, however, was impractical for FSD particles, owing to the small amount of mass that could be sampled and the high probability of deterioration during the polishing step. Therefore, in this study, FSD was deposited on polycarbonate filters (SKC, Pittsburgh, PA, USA), which were attached on stubs using vacuum pumps (AirChek 52, SKC) (Gasparon *et al.*, 2016). Subsequently, these stubs received conductive carbon film for the dissipation of

electrical charge and the heat released by the sample exposure beam SEM electrons. The method was set to read approximately 35,000 particles of FSD.

An advantage of this method is that MLA has automated de-agglomeration function that detects particles agglomeration and separates them (Frandrigh *et al.*, 2007). Although some precautions are conducted to prevent this issue during the sample preparation, particles easily touch each other and this can lead to biased results.

### **3.2.5 Transmission electron microscopy (TEM)**

One FSD sample (CP1) was selected for TEM analyses to obtain a better understanding of the mixed phases identified by MLA analyses. This sample presented the highest number of As-bearing mixed phase particles in the study. Suspension of samples was achieved by dispersion in ethanol in Eppendorf tubes and by sonication in an ultrasound bath for 3 min. A drop of each suspension was placed on distilled water in a Petri dish to form a Langmuir film of dispersed particles on the water surface. Subsequently, the carbon film side of the C-coated TEM Cu-grid (300 mesh) was placed in contact with the fine particles spread on the water surface to pick up the solids by capillarity effect. The samples were analyzed by high resolution TEM (HRTEM), STEM, and EDS. The analyses were performed using a LaB6-TEM Tecnai G2-20 (FEI), operating at 200 kV, equipped with a 30 mm<sup>2</sup> window Si(Li) EDS detector (EDAX).

## **3.2.6 RESULTS AND DISCUSSION**

### **3.3 Gastrointestinal BAC**

Mean and median As concentrations surface dust samples collected in two surveys (dry and wet seasons) were  $200 \pm 170$  (n = 14) and 168 mg/kg, respectively, with a range of 6-568 mg/kg (Table 3.6). The mean values were similar for both surveys. The mean and median bioaccessible As concentrations were  $4.7 \pm 4$  and 4 mg/kg. The mean BAC ranged from  $2.9 \pm 2\%$  to  $3.8 \pm 2\%$  for wet and dry seasons, respectively. The BAC values ranged from 1.1 to 8.3% for the different locations. This variability is not unusual for this type

of sample and reflects similar physical and chemical composition of the samples. Although the surface dust samples are not usually used for risk assessment for Brazilian regulatory purposes (as soil samples from 0 to 20 cm are required), values of the current study may be more representative of As exposure to ingestion, as they provided direct information regarding As concentrations and BAC in the outdoor urban dust. BAC values for surface dust were consistent with those obtained by Ono *et al.* (2012), who reported BAC in a range from below detection limit to 4.2% for soil and tailings samples collected in the same area of study. In the same region as the present investigation, our group determined BAC values within a range of 0.3–5.0% in soil samples (size fraction  $\leq 250$   $\mu\text{m}$ ) containing As concentrations ranging from 211 to 4,304 mg/kg (Ciminelli *et al.*, 2018). In comparison, Meunier *et al.* (2010) reported BAC values as high as 49% measured in gold mining tailings containing amorphous Ca-Fe arsenates, whereas samples containing arsenopyrite or scorodite exhibited BAC values  $< 1\%$ .

Table 3.6: Arsenic concentration and bioaccessible arsenic of surface dust samples collected in residential areas (fraction  $\leq 250 \mu\text{m}$ ).

Sample	As content (mg/kg)		Bioaccessible As (mg/kg)		As Bioaccessability (%)	
	Dry Season	Wet Season	Dry Season	Wet Season	Dry Season	Wet Season
H1	6	14	0.5	0.9	8.3	6.4
H2	461	568	14.8	8	3.2	1.4
H3	186	136	5.4	2.2	2.9	1.6
H4	321	357	5.8	5.4	1.8	1.5
H5	53	56	1.9	2.5	3.6	4.5
H6	166	101	8.5	3.8	5.1	3.8
H7	211	169	3.8	1.9	1.8	1.1
Mean $\pm$ SD	201 $\pm$ 155	200 $\pm$ 196	5.8 $\pm$ 5	3.5 $\pm$ 2	3.8 $\pm$ 2	2.9 $\pm$ 2
Median	186	136	5.4	2.5	3.2	1.6
Range	6 - 461	14 - 568	0.5 - 14.8	0.9 - 8	1.8 – 8.3	1.1 – 6.4
Mean $\pm$ SD	200 $\pm$ 170		4.7 $\pm$ 4		3.4 $\pm$ 2	
Median	168		4		3.1	
Range	6 - 568		0.3 – 14.8		1.1 – 8.3	

### 3.4 Lung BAC

Bioaccessible As and As concentrations of FSD samples are presented in Table 3.7. Mean BAC was relatively low for residential samples ( $2.7 \pm 0.1\%$ ) and ranged from 1.6 to 3.5% to afford bioaccessible arsenic of 1.0 (H5) to 7.6 mg/kg (H6), with a mean of  $5.6 \pm 3$  mg/kg. No apparent correlation was observed between the magnitude of bioaccessible As and BAC. Arsenic concentrations for the five residential FSD samples ranged from 32 (H5) to 445 mg/kg (H2). Sample H5 was originally located in an upwind position of the gold mine where there is no gold mineralization and represents a control point and the lowest As concentration.

Table 3.7: Arsenic concentration and lung BAC in FSD samples ( $\leq 10 \mu\text{m}$ ).

Sample	As content (mg/kg)	Bioaccessible As in simulated lung fluid (mg/kg)	BAC (%)
H2	445	7.3	1.6
H5	32	1.0	3.3
H6	216	7.6	3.5
H17	212	5.6	2.6
H19	265	6.7	2.5
Mean $\pm$ SD	$234 \pm 147$	$5.6 \pm 3$	$2.7^* \pm 1$
Median	216.73	6.7	2.6
CP1	655	27.2	4.2
CP2	279	7.7	2.8
Mean $\pm$ SD	$467 \pm 266$	$17.4 \pm 14$	$3.5^* \pm 1$

\*Mean BAC represents the mean of all BAC values listed in above.

The mean BAC and As concentration for the two CP samples was  $3.5 \pm 1\%$  and  $467 \pm 266$  mg/kg, respectively. Although there was a difference in the As concentration between residential and CP samples, BAC appeared to be consistent in value. Bioaccessible As from SLF for CP samples ranged from 7.7 (CP2) to 27.2 mg/kg (CP1). This difference may reflect the different mineralogy of the ore processed in the two crushers, with the ore



in CP2 being richer in sulfides compared that in CP1, which derived from a softer near-surface ore. Other mechanisms may also account for this difference, such as the presence of Fe oxy-hydroxides. These two hypotheses are further addressed in Section 3.5. Despite the mineralogical differences, residential FSD and dust from crusher areas showed similar and relatively low BAC values (2.7% and 3.5%, respectively). The partition of As in the different mineral phases varied quite significantly in the two industrial dust samples (with different BAC) and industrial dust samples/residential FSD (similar BAC), as was further confirmed by the microscopy analyses. These results are consistent with the low BAC of all As-carriers.

The literature shows marked variability of As BAC in SLFs. Considering the different particle size fractions and high variability in the SLF used in similar investigations, comparisons among published studies should be viewed with a degree of caution (Martin *et al.*, 2018). Wizeman and Zereini (2014) found BAC of 57% (ranging from 27 to 73%) using Gamble's solution (pH 7.4) in airborne PM<sub>10</sub> samples from Frankfurt, Germany whereas Huang *et al.* (2014b) reported As BAC of 29.88% using lung simulating serum for household PM<sub>2.5</sub> samples in urban centers of Guangzhou, China. The differences are a result of the different As-bearing particles, sources, and likely the variety of the simulated lung solutions.

Even in mining influenced areas, BAC values may vary significantly depending on the mineral deposits. Whereas the BAC for residential and dust from ore samples in the present study was within 1.6 – 4.2%, those reported by Kim *et al.* (2014) for soil samples (sieved to a fraction <20 µm) showed a range of 2.1 to 46.9% when using phagolysosomal simulant fluid with a relatively lower pH of 4.5. Drahotka *et al.* (2018) reported lung As BAC ranging from 5.3 to 5.9% in mine waste, urban soil, and road dust samples among particle sizes <11 µm from the Czech Republic. The lowest As BAC was presented by Martin *et al.* (2018), where in the results ranged from 0.020 to 0.036% in particle sizes <20 µm in a historical mine in Australia. Although samples presented high As concentrations (1220 – 19,800 mg/kg), the authors attributed the low BAC to the presence of insoluble As-bearing minerals, such as scorodite. Together, these findings illustrated

that BAC is mostly influenced by mineral composition and association. Therefore, a better understanding of these differences is necessary.

### **3.5 Identification of main mineral phases and As-bearing phases**

The MLA was employed as a tool to identify the mineral phases in the FSD and BP samples. The identification of a given mineral phase by MLA is performed by matching its spectrum with a mineral library, a pre-defined list of minerals and non-minerals phases. This mineral library, prepared prior to the automated analysis, comprises a collection of high-quality spectra of phases identified in the sample, usually validated by X-ray diffraction-XRD and other analyses. The building of a standards library directly from the sample ensures that the instrument parameters, such as beam energy, are consistent (Fandrich *et al.*, 2007). A total of 35 minerals (including minerals, metal fragments and organic matter) reflects a robust survey on mineral phase identification during this and previous works of our group in the region. This procedure also allows a good reading resolution of particles with diameter  $\leq 10 \mu\text{m}$ .

The main constituents found in FSD samples were the muscovite/clay minerals and quartz, silicate minerals, Fe oxy-hydroxides, carbonates and carbonaceous matter. The latter was identified by a typical morphology of non-mineral phases as well as major carbon associated with low concentrations of elements such as Si, Al, and Mg (Table 3.8: Main mineral phases weight (%) identified in FSD and BP samples by MLA analyses.). The main feature of the ore sample (BP) was the presence of significant amounts of sulfide minerals, such as pyrite and arsenopyrite.

The MLA technique also allows for the identification of the sample constituents present in trace amounts whereas XRD analysis identifies constituents above 1–3%. Table 3.9 shows the number of particles of sulfide and As-bearing phases identified by MLA in FSD. The results of FSD composition were compared with that representing a typical ore sample (BP). Sulfides were more representative in the CP2 sample among FSD samples (226 out 35,624 particles), which is consistent with dust collected in the crusher area of the sulfide ore. Arsenic was found in the following phases: (i) arsenopyrite, (ii) scorodite

(iii) iron oxy-hydroxide, (iv) mixed phases, and (v) muscovite/clay. Arsenopyrite was identified in H2, H19, CP1, and CP2 in relatively low amount (maximum nine particles), showing that the presence of this sulfide in FSD samples and its contribution to bioaccessible As in FSD was not significant. The same conclusion applies to scorodite, which was identified mostly in CP1 (16 out 36,703 particles) and is unlikely the main mineral that regulates the As BAC among the samples tested.

Arsenic-bearing iron oxy-hydroxides were identified as the major As-bearing phase in all FSD samples, suggesting this phase may be the key driver regulating As solubility in SLF. Beak *et al.* (2006) found As BAC of  $\leq 5\%$  for the As-bearing iron oxy-hydroxide phase in a model soil mineral (ferrihydrite). This finding is consistent with the As BAC values reported in the present study (3.5 and 2.7% for dust from ore and residential samples, respectively). As-bearing mixed phases also appeared to comprise a significant group for As-bearing phases, owing to the relatively large number of particles identified for all samples. According to the EDS analysis, these phases were characterized by the presence of Al (2.44–47.31%), Si (1–4.02%), P (0.47–34.29%), Ca (0.47–7.34%), Fe (0.18–23.60%), As (0.06–7.23%), Ba (0.11–6.01%), Pb (0.14–25.64%), and O (50.67–78.80%) as the main constituents, whereas Na, Ti, Cl, S, K, V, Cr, Cu, Sr, and Cd appeared as minor factors. Because of the complex elemental composition, no specific known mineral phase could be assigned to these apparent mixed phases during the MLA analysis. Galena was found in high number across most of the samples, which suggests that this phase is natural in the area.

Table 3.9 also shows the analyses of the ore sample (BP). Pyrite represented the main constituent of the BP sample (277 out 33,328 particles) among other sulfide minerals. Arsenopyrite was the second major constituent of this sample followed by pyrrhotite (94 and 79 particles, respectively). The differences between the ore and FSD samples were evident. Whereas iron oxy-hydroxides and the mixed phases comprised the main As-bearing phases in FSD, and arsenopyrite appeared as a rare constituent, this sulfide constituted the main As-bearing phase in the ore. To better investigate the features of arsenopyrite particles in the ore, the BP sample was separated into sub-samples with different particle sizes through use of a cyclone-based classifier. MLA was then employed

to identify the main trace elements in the different fractions generated by the cyclones (Table 3.10).

Figure 3.4 demonstrates that arsenopyrite clearly concentrated in the underflow of the first cyclone (667 particles with sizes  $>39.3 \mu\text{m}$  in first cyclone underflow, compared to 94 particles in BP). The number of particles of arsenopyrite was reduced significantly with the decrease in particle size, with only 14 particles with particle sizes below  $11.1 \mu\text{m}$  being identified. It was possible to infer, as arsenopyrite was mostly present in particle sizes  $>10 \mu\text{m}$ , that its contribution to the As in FSD was minor or negligible. This size feature combined with the relatively high density rendered arsenopyrite not easily transported by the wind in dust. Therefore, although the mining operation is very close to the city the heavy and relatively coarse sulfide minerals were not expected to be frequently found in the FSD samples. This hypothesis is supported by the data shown in Table 3.9.

Table 3.8: Main mineral phases weight (%) identified in FSD and BP samples by MLA analyses.

<b>Main mineral phases</b>	<b>H2</b>	<b>H5</b>	<b>H6</b>	<b>H17</b>	<b>H19</b>	<b>CP1</b>	<b>CP2</b>	<b>BP</b>
Muscovite/Clays	66.5	45.4	83.8	58.1	56.5	86.3	85.0	49.9
Quartz	18.2	23.9	8.9	7.9	12.0	10.4	9.7	18.6
Fe oxy-hydroxides <sup>i</sup>	3.8	3.9	1.9	4.6	9.4	2.0	1.6	0.7
Carbonaceous matter	2.6	1.7	2.0	5.2	4.0	0.5	0.4	0
Other Silicates <sup>ii</sup>	3.1	20.7	2.2	14.2	10.3	0.4	2.1	8.6 <sup>iv</sup>
Carbonate	2.7	1.6	0.2	7.2	5.8	0.1	0.1	3.6
Others <sup>iii</sup>	3.1	2.8	1.0	2.8	2.0	0.3	1.1	18.6 <sup>v</sup>
<b>Total</b>	<b>100</b>	<b>100</b>	<b>100</b>	<b>100</b>	<b>100</b>	<b>100</b>	<b>100</b>	<b>100</b>

<sup>i</sup> Including Fe oxy-hydroxides with arsenic.

<sup>ii</sup> Feldspar, tourmaline, zircon, orthosilicate.

<sup>iii</sup> Sulfides (pyrite, chalcopyrite, galena, spharelite, arsenopyrite), As-bearing mixed phases, scorodite, apatite, monazite, anhydrite, cassiterite, talc, ilmenite, clinocllore, copper, zinc, nickel, anatase, barite.

<sup>iv</sup> Albite, chlorite, orthoclase, biotite, tourmaline, zircon.

<sup>v</sup> Sulfides (17.3% of arsenopyrite, pyrite and pyrrotite) and others (apatite, ilmenite, anatase, monazite, among other trace minerals).

Table 3.9: Trace constituents of sulfide and arsenic-bearing phases identified by MLA in FSD and BP samples.

<b>Sulfides and As bearing phases</b>	<b>H2</b>	<b>H5</b>	<b>H6</b>	<b>H17</b>	<b>H19</b>	<b>CP1</b>	<b>CP2</b>	<b>BP*</b>
Pyrite (FeS <sub>2</sub> )	8	4	0	12	10	1	115	277
Chalcopyrite (CuFeS <sub>2</sub> )	1	1	0	1	0	0	13	7
Galena (PbS)	29	19	14	42	40	2	82	3
Spharelite (ZnS)	0	5	0	15	13	0	7	5
Pyrrhotite (Fe <sub>(1-x)</sub> S)	0	0	0	0	0	0	0	79
Arsenopyrite (FeAsS)	1	0	0	0	1	1	9	94
Scorodite (FeAsO <sub>4</sub> )	1	1	1	3	2	16	10	0
As bearing Fe oxy-hydroxides	568	396	155	330	371	470	154	42
As bearing mixed phases	22	33	60	74	39	165	56	48
As bearing Muscovite/Clays	0	1	1	0	0	1	0	0
<b>Total of sulfide mineral phases</b>	<b>39</b>	<b>29</b>	<b>14</b>	<b>70</b>	<b>64</b>	<b>4</b>	<b>226</b>	<b>465</b>
<b>Total of As bearing phases</b>	<b>592</b>	<b>431</b>	<b>217</b>	<b>407</b>	<b>413</b>	<b>653</b>	<b>229</b>	<b>184</b>
<b>Total of particles analyzed</b>	<b>36,856</b>	<b>36,449</b>	<b>35,584</b>	<b>35,144</b>	<b>38,517</b>	<b>36,703</b>	<b>35,624</b>	<b>33,328</b>

\*Values normalized based on total number of particles for comparison

Table 3.10: Trace constituents of sulfide and arsenic-bearing phases identified by MLA in different sizes of BP samples.

Sulfides and As bearing phases*	BP	Cyclone 1	Cyclones 2 - 5	Cyclone 5
		C1_UF**	C2-5_UF**	C5_OF***
	Particle size ≤150 μm	Particle size >39.3 μm	Particle size 11.1 – 39.3 μm	Particle size <11.1 μm
Pyrite (FeS <sub>2</sub> )	277	2,151	188	110
Chalcopyrite (CuFeS <sub>2</sub> )	7	41	2	1
Galena (PbS)	3	27	1	0
Sphalerite (ZnS)	5	11	1	0
Pyrrhotite (Fe <sub>(1-x)</sub> S)	79	166	47	14
Arsenopyrite (FeAsS)	94	667	102	14
Scorodite (FeAsO <sub>4</sub> )	0	0	0	0
As bearing Fe oxy-hydroxides	42	44	3	1
As bearing mixed phases	48	0	0	34
As bearing Muscovite / Clays	0	0	0	0
Total of sulfide mineral phases	465	3,063	341	140
Total of As bearing phases	184	711	105	49
Total of particles analyzed	33,328	33,159	33,360	33,841

\*Values normalized based on total number of particles for comparison

\*\* Cyclone Underflow; \*\*\* Cyclone Overflow.

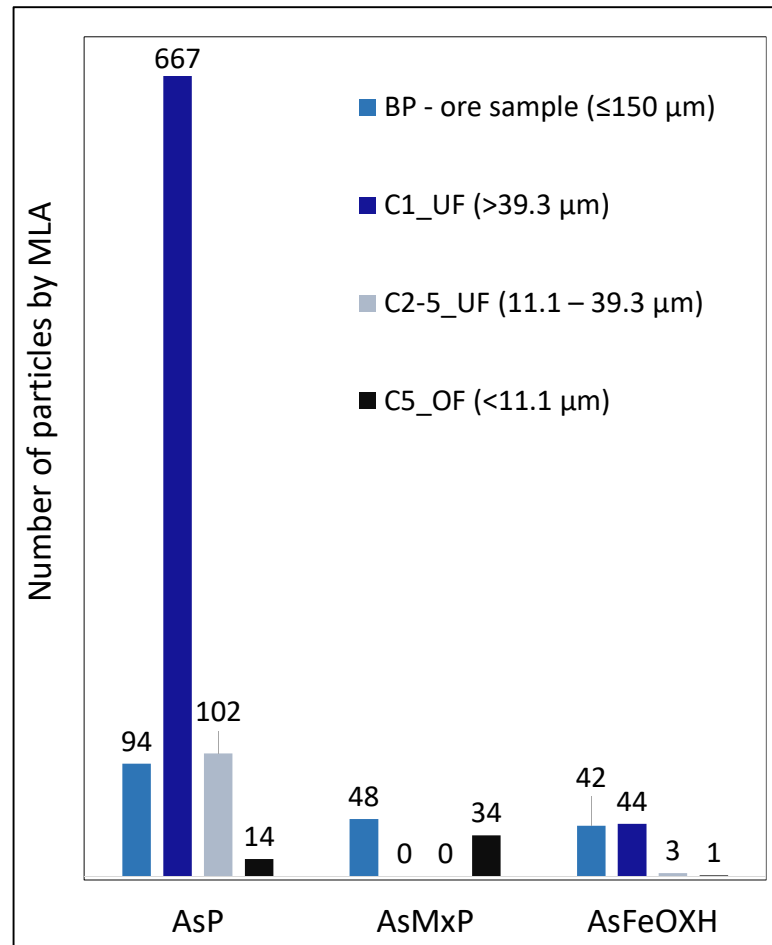


Figure 3.4: Trace constituents of arsenic-bearing phases identified by MLA in the as-received ore (BP) sample and in the different size fractions (AsP: arsenopyrite; AsMx: As bearing mixed phases; AsFeOXH: As bearing Fe oxy-hydroxides).



An excellent correlation ( $R^2 = 0.98$ ) was obtained by comparing elemental concentrations determined by MLA (polished sections, BP samples) with chemical analyses made by EDX (Al, Si), Leco (S) and ICP-OES (Fe, As) (Figure 3.5). The preparation of polished sections for a quantitative MLA analyses was not possible due to the fine particle size of the FSD samples. A comparison of elemental concentrations obtained by MLA (loose particles on filters, FSD) and chemical analyses is shown in Figure 3.6. Arsenic concentrations are below 0.1% and therefore lower than the level recommended for quantitative EDX analyses. Nevertheless, the MLA technique allowed for the identification of As-bearing phases from a significant population of particulate material (up to 38,000 particles), in a heterogenous, complex mineral assembly, which would not have been possible by the typical particulate analyses. The refinement of the method for quantitative analysis of particulate matter is under development.

Figure 3.7 presents BSE images of typical mineral phases in FSD samples. The particle sizes were consistent with the sample features ( $<10 \mu\text{m}$ ). The solids were well distributed in the filter, which facilitated their identification via the contrast provided by the BSE images.

High spatial resolution to assess the mineralogy of the mixed phases was achieved using transmission electron microscopy (TEM). These mineral phases were identified by HRTEM image analysis and selected area electron diffraction (SAD) (Figure 3.8 and Figure 3.9). The results showed that mixed phases were essentially an assembly of As-bearing hematite and goethite nanocrystals often entangled with phyllosilicates, and thus forming larger particles of few hundreds of nanometers (Figure 3.8a,b). Aluminum was often present in the iron oxy-hydroxide phases. The presence of phyllosilicates may explain the occurrence of other metals, P and Si, observed in the SEM-EDS data. The interaction volume (of only a few micrometers in size), where the X-rays are emitted from the sample, is much larger than the probe size in SEM. Therefore, X-ray signals from other particles around the target are generated.

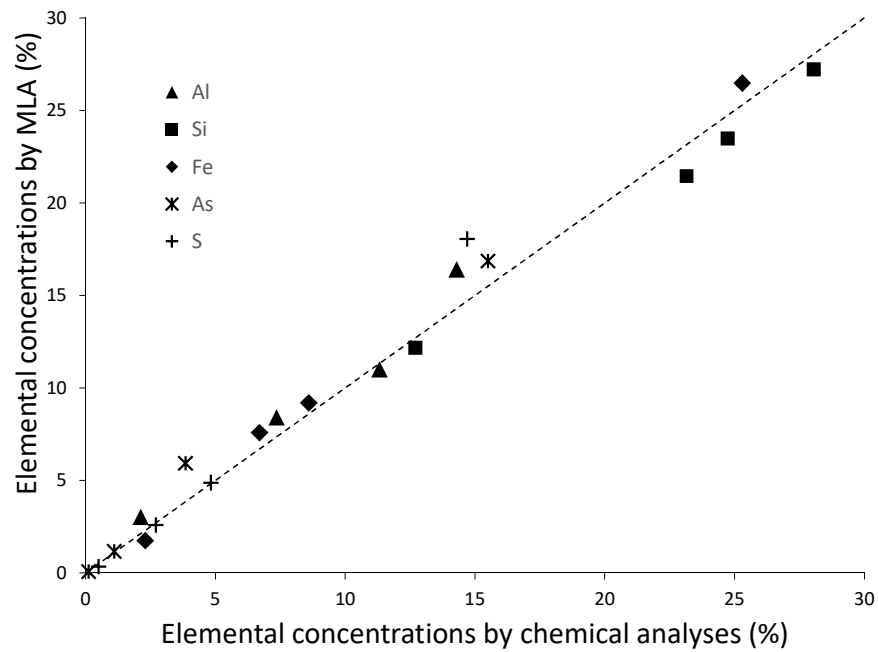


Figure 3.5: Elemental concentrations determined by MLA and EDX (Al, Si), Leco (S) and ICP-OES (Fe, As) in BP samples.

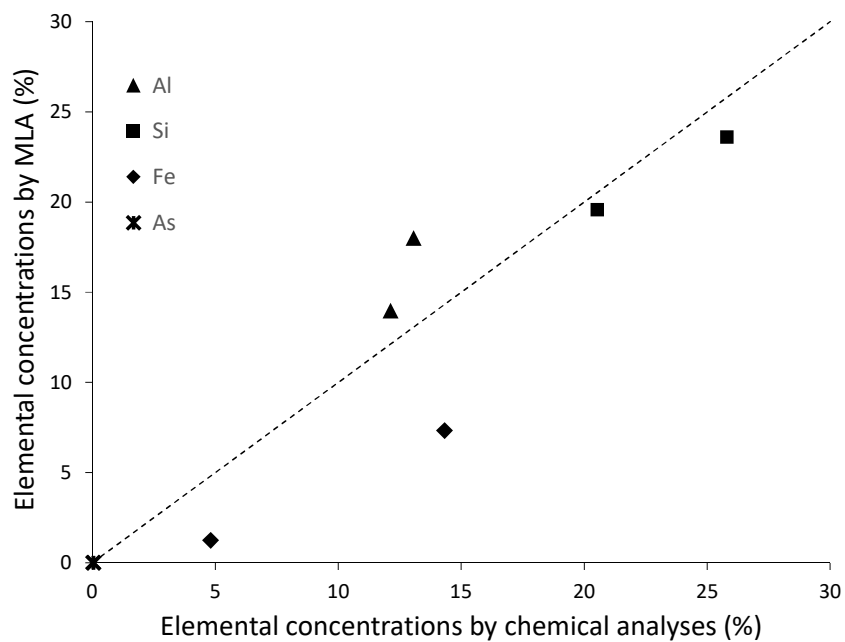


Figure 3.6: Elemental concentrations determined by MLA and EDX in FSD samples (H2 and H19).

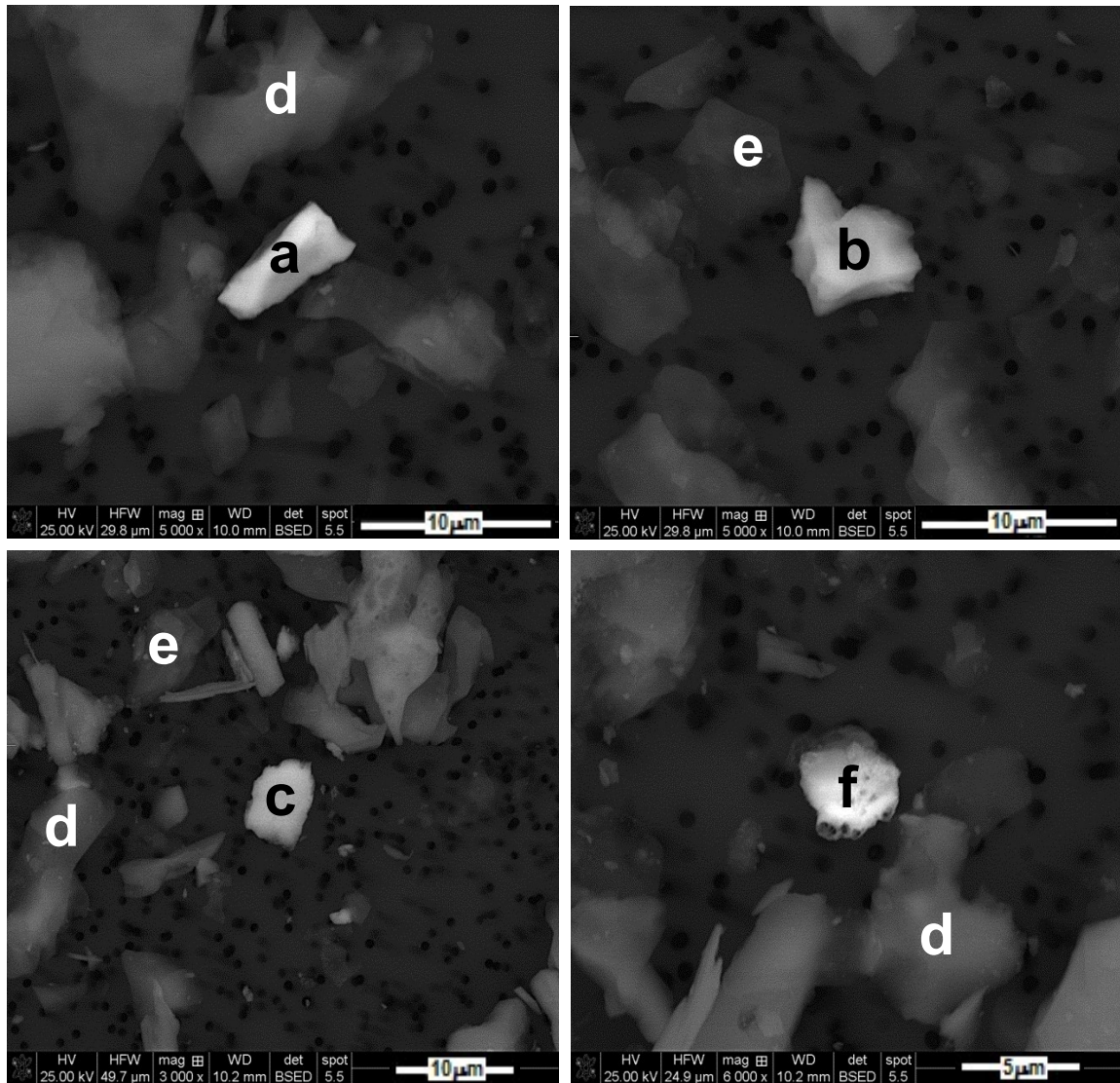


Figure 3.7: Backscattered electron (BSE) images of mineralogical phases and elemental analyses (EDS) of main constituents of FSD\*.

\* (a) arsenopyrite (15.7%S; 34.4%Fe; 49.9%As); (b) pyrite (51.8%S; 48.2%Fe); (c) Fe oxyhydroxide with As (1.5%Al; 63.3%Fe; 3.8%As; 31.4%O); (d) muscovite (20.3%Al; 21.6%Si; 9.9%K; 48.2%O); (e) clay minerals (21.0%Al; 22.5%Si; 56.5%O); (f) arsenic bearing mixed phases (7.23%As and others: Al; Si; P, Fe, Ti, K, Pb, O).

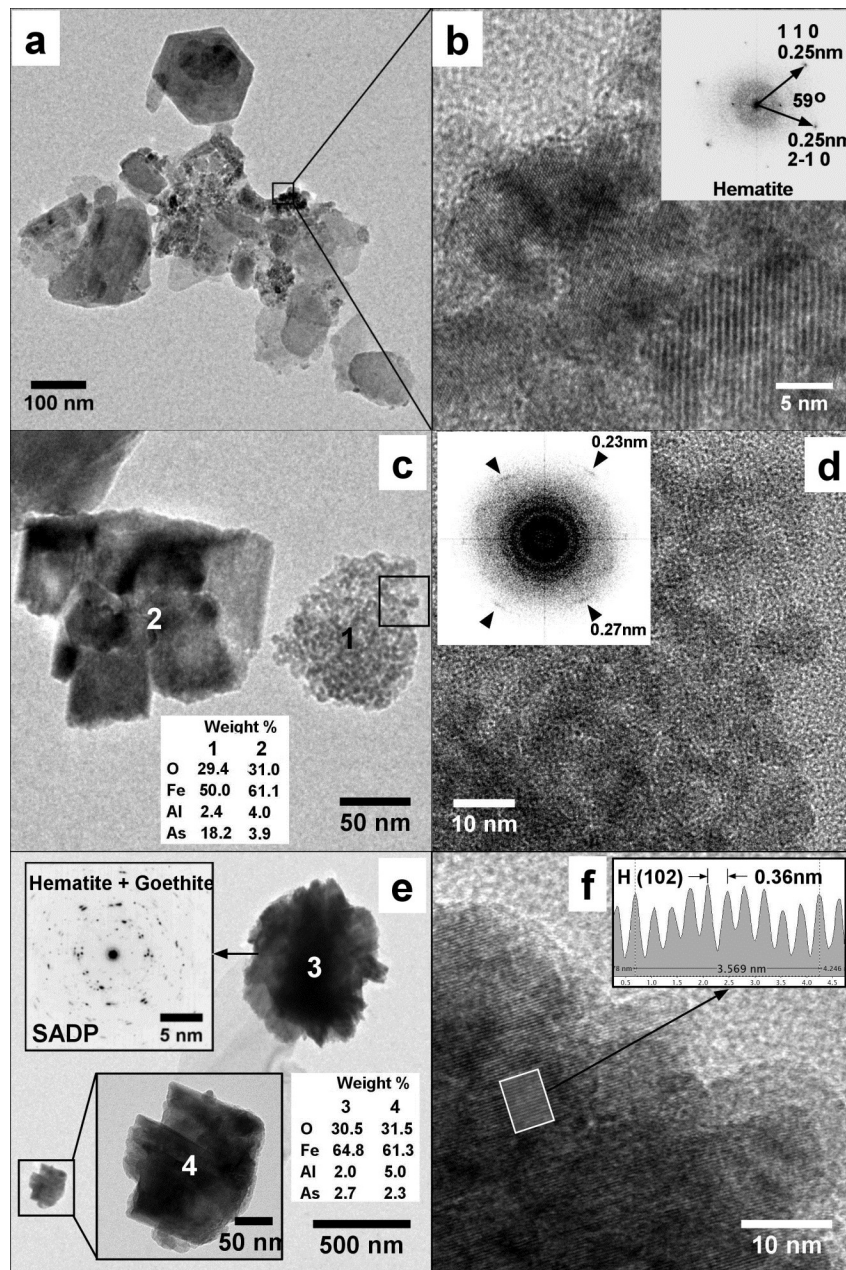


Figure 3.8: Transmission electron microscopy images of CP1 sample\*

\* (a) phyllosilicates entangled with oriented aggregates of nanostructured hematite shown in detail in (b). The inset in (b) shows the measured lattice fringes of hematite; (c) and (e) show the bright field images of particles 1 to 4, and their respective elemental composition by EDS; (d) and (f) show the HRTEM images of particles 1 and 3, respectively. The inset in (d) shows the FFT of the HRTEM image and the black arrows point the spots that correspond to the lattice fringes 0.23 nm and 0.27 nm of ferrihydrite. The inset at top left side in (e) shows the SAD pattern (SADP) taken from the particle 3, which has both hematite and goethite nanoparticles in there. The inset in (f) shows the line profile across the marked rectangle whose interatomic distance corresponds to the d-space of the (102) planes for hematite.

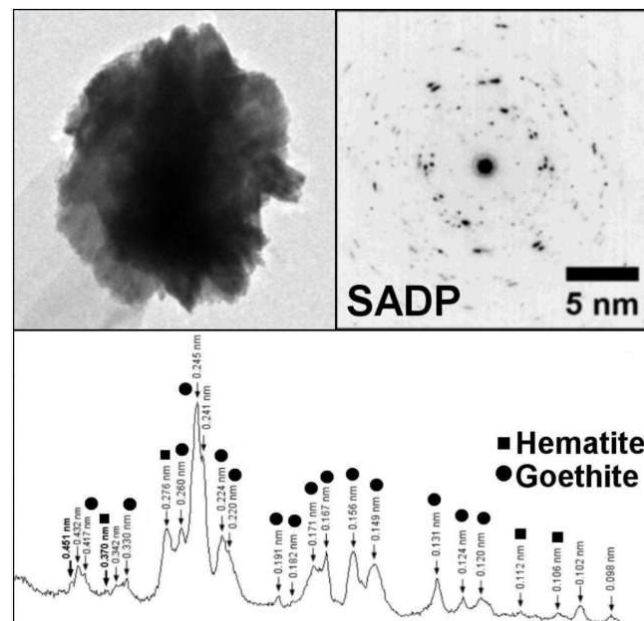


Figure 3.9: SAD analyses demonstrating the presence of hematite and goethite in CP1 sample.

The STEM-EDS indicated larger amounts of As (up to 18.2 wt%) in the nanoparticle aggregate, which was likely comprised of hematite (Figure 3.8b,c). Although the EDS quantification of the nanoparticle aggregate (Figure 3.8c) showed a lower Fe content (50.0 wt%) relatively to  $\alpha$ -Fe<sub>2</sub>O<sub>3</sub>, the HRTEM image analysis suggested that the aggregate consisted of hematite nanoparticles. Consistent with this, the measured lattice fringes of 0.23 and 0.27 nm on the Fast Fourier Transform (Figure 3.8d) were assigned to the hematite  $d_{hkl}$  planes (104) and (113), respectively. The results showed relatively lower As content (2.3 to 3.9 wt%) in the mixed phases.

In summary, our results suggest that the source of As in FSD may be mainly related to the soils typically found in the region of study. Ciminelli *et al.* (2018) identified the predominance of similar As bearing phases in soil samples collected in the same region, in areas with no evidence of previous anthropogenic activities. Investigation conducted using TEM analyses showed that As-bearing iron oxyhydroxides are formed by nanoaggregates of goethite and hematite (Ciminelli *et al.*, 2018), which is the same association pattern identified in the present investigation.

### **3.6 Health risk assessment (HRA) associated with As intake from inhalation and ingestion of FSD and surface dust**

Health risk assessment was used as a tool to evaluate the potential risk associated with As exposure. The As intake and predicted cancer risk for adults from both inhalation and oral ingestion are presented in Table 3.11. Maximum and median values were considered for this assessment and calculations followed the guidelines established by the Brazilian Ministry of Health (2010) and ATSDR (2005). The aim was to evaluate the HRA of As exposure for the Paracatu population living in the surroundings of the mining area. Data from Ciminelli *et al.* (2017) were also considered for the HRA evaluation as they provide As intake from the ingestion route including food and water in the area of study. In summary, As intake from FSD was based on the inhalation of 22 m<sup>3</sup> of air (mean between male and female), soil ingestion of 50 mg/day, and body weight of 70 kg. No in situ measurement of airborne PM<sub>10</sub> dust was employed in the present study; thus, the concentration used to calculate the total dust daily intake was that specified by the

Brazilian legislation, which considers the maximum value of  $120 \mu\text{g}/\text{m}^3$  in 24 h for dust (BRAZIL, 2018). The same method was used as published by Drahota *et al.* (2018).

Risk assessment calculations were carried out by comparing the total As intake to the Benchmark Dose Lower Confidence Limit (BMDL) and As cancer slope factor (CSF). JCEFA (2011) established that the inorganic As BMDL for an increase of 0.5% of lung cancer incidence is  $3.0 \mu\text{g}/\text{kg}(\text{b.w})/\text{day}$  ( $\text{BMDL}_{0.5}$ ), ranging from 2.0 to  $7.0 \mu\text{g}/\text{kg}(\text{b.w})/\text{day}$  based on epidemiological data. The linear dose relationship for As CSF, which was calculated following guidelines established by USEPA (1995), reported the risk of  $1 \times 10^{-6}$ ,  $1 \times 10^{-5}$ ,  $1 \times 10^{-4}$  as the probability of one additional case of cancer in an exposed population of 1,000,000, 100,000, and 10,000, respectively. In Brazil, the tolerable risk for carcinogenic substances is one additional case of cancer in 100,000 population ( $1 \times 10^{-5}$ ) (BRAZIL, 2009). This CSF approach tends to be less appropriate than BMDL, when considering that the provisional guideline value of  $10 \mu\text{g}/\text{L}$  As in drinking water established by WHO (2011) predicted a cancer risk of  $4.29 \times 10^{-4}$ , which is already slightly in excess of the so-called acceptable risk of  $1 \times 10^{-6}$  to  $1 \times 10^{-4}$ .

Table 3.11: Arsenic intake from surface dust and FSD.

Pathway	iAs intake ( $\mu\text{g}/\text{kg}(\text{b.w})/\text{day}$ )	% intake (A1; B1)	% intake (A2; B2)	Predicted cancer risk
A1: Inhalation FSD (max As BAC: $7.6 \text{mg}/\text{kg}$ ; $0.91 \text{ng}(\text{As})/\text{m}^3$ )	0.00029	0.1	-	$3.92 \times 10^{-6}$
A2: Inhalation FSD (median As BAC: $6.7 \text{mg}/\text{kg}$ ; $0.80 \text{ng}(\text{As})/\text{m}^3$ )	0.00025	-	0.1	$3.44 \times 10^{-6}$
B1: Surface Dust (max As BAC: $14.8 \text{mg}/\text{kg}$ )	0.01057	5.2	-	$1.59 \times 10^{-5}$

B2: Surface Dust (median As BAC: 4.0mg/kg)	0.00286	-	1.5	$4.29 \times 10^{-6}$
C: Water (0.21µg/L)*	0.00600	2.9	3.0	$9.00 \times 10^{-6}$
D: Food*	0.18800	91.8	95.4	$2.82 \times 10^{-4}$
Total (A1, B1, C, D)	0.20486 (6.8% of BMDL0.5)	100	-	$3.11 \times 10^{-4}$
Total (A2, B2, C, D)	0.19711 (6.6% of BMDL0.5)		100	$2.99 \times 10^{-4}$
BMDL0.5	3.0			
CSF oral	1.5mg/kg(b.w)/day			
CSF inhalation	$4.3 \times 10^{-3}$ per µg/m <sup>3</sup>			
Water (10µg/L)	0.28571			$4.29 \times 10^{-4}$
Tolerable risk for carcinogenic substances - local legislation (BRAZIL, 2009)				$1 \times 10^{-5}$

\*Ciminelli *et al.* (2017)



Considering that the maximum allowed daily level of particulate matter is  $120 \mu\text{g}/\text{m}^3$  (BRAZIL, 2018) for inhaled dust ( $\leq 10 \mu\text{m}$ ) in the area of the study, the total dust daily intake for an adult reaches a maximum  $2,640 \mu\text{g}/\text{day}$  ( $120 \mu\text{g}/\text{m}^3 \times 22 \text{m}^3$ ). Referring to the maximum and median concentrations of bioaccessible As in the residential FSD samples (7.6 and  $6.7 \text{mg}/\text{kg}$ ), the total As intake becomes 0.00029 and  $0.00025 \mu\text{g}/\text{kg}(\text{b.w})/\text{day}$ , respectively. The corresponding inhalation is 0.91 and  $0.80 \text{ng}/\text{m}^3$ , respectively.

Following the same rationale for surface dust samples, As daily intake by oral ingestion would be 0.01057 and  $0.00286 \mu\text{g}/\text{kg}(\text{b.w})/\text{day}$  for maximum and median bioaccessible As values. These results agree with those reported by Ciminelli *et al.* (2018) with soil samples. The findings also indicated that the relative risk regarding As exposure by inhalation and oral ingestion was low in the region of study ( $0.00029$  and  $0.01057 \mu\text{g}/\text{kg}(\text{b.w})/\text{day}$ ) when compared with the  $\text{BMDL}_{0.5}$  of  $3 \mu\text{g}/\text{kg}(\text{b.w})/\text{day}$  and the total As intake.

Additional information presented by Ciminelli *et al.* (2017) was used to calculate the total As intake considering also food and water intake. It should be noted that there were only a few generally consumed food items produced locally (e.g. vegetables). However, people in Paracatu consumed a wider variety of food, such as rice, not produced locally. Previous study (Ciminelli *et al.*, 2017) reported the arsenic intake by Paracatu community from food ingestion considering common sources of food items.

The present study focused on the geogenic exposure to the local population which derived mostly if not exclusive from the local environment. The area is geochemically defined by a natural strong As anomaly (Mello *et al.*, 2006). The resuspension and dissemination of mineral particles in the atmosphere is the direct consequence of the erosion of As-rich sediments and soils, and this process is amplified by any activity that causes disturbance of the regolith, such as land clearance, mining, construction work, agriculture, vehicular traffic on unpaved roads. Considering all sources, the total As intake was  $<7\%$  of the  $\text{BMDL}_{0.5}$  ( $0.205$  and  $0.197 \mu\text{g}/\text{kg}(\text{b.w})/\text{day}$ ). Food contribution constitutes the main source of As intake ( $>90\%$ ), following the worldwide trend reported in non-endemic areas (JECFA, 2011).

## 4 CONCLUSIONS

Dust samples were collected in the proximity of an important geological arsenic anomaly that is also influenced by gold mining activities. Gastrointestinal and lung BAC tests yielded low bioaccessible concentrations of As in surface soil and residential FSD samples ( $3.4 \pm 2\%$  and  $2.7 \pm 1\%$ , respectively). Mineralogical assessment using MLA for the FSD samples demonstrated that arsenic was mainly associated with hematite and goethite nanoparticles. The As-bearing iron oxy-hydroxides phase was the major As-bearing phase in all samples (app. 70-90%), revealing that this phase may be regulating the As solubility in the SLF. These are the typical As-bearing phases found in soil samples in the region of study, as reported in previous investigations of our group (Ciminelli *et al.*, 2018). As-bearing mixed phases (where As is also associated with Fe oxy-hydroxides nanoparticles mixed with other phases) also comprised a significant phase present in the FSD samples that might limit the As solubility in the SLF. TEM analyses demonstrated that this phase is composed of nanocrystals formed by hematite and goethite that are entangled to phyllosilicates, forming larger particles of several hundred nanometers. The low As solubility in FSD samples was related to arsenic fixation in these iron oxy-hydroxide nanoparticles.

Ore sample was demonstrated to have different mineralogy from FSD samples, as its main As-bearing phase was arsenopyrite. Size separation of an ore sample showed that the number of arsenopyrite particles decreased significantly with the decrease of particle size and therefore this mineral is not expected to be found in large amounts in FSD. The source of arsenic in FSD was rather related to the typical soils in the region of study.

Health Risk Assessment demonstrated that As intake from both FSD inhalation and surface dust ingestion was relatively low (<10%) compared to the total As intake and BMDL<sub>0.5</sub> of  $3.0 \mu\text{g}/\text{kg}(\text{b.w})/\text{day}$ , thus confirming that the risk associated with the combined As exposure of inhalation and oral dust ingestion could be considered low in the region of the study

## 5 CONSIDERAÇÕES FINAIS

A exposição ao arsênio e os consequentes riscos para a saúde humana representam uma preocupação comum para as populações que vivem próximas a minerações de ouro que possuem minerais contendo arsênio. Até onde sabemos, este estudo é o primeiro trabalho a quantificar os níveis de arsênio bioacessível associado a poeira inalável e, ao mesmo, tempo identificar as fases portadoras a partir da identificação estatisticamente robusta de partículas individuais, através de técnicas utilizando microscopia eletrônica de varredura com sistema de análise de imagens, posteriormente refinada com as análises das estruturas em escala nanométrica, através da microscopia de transmissão.

Os resultados obtidos mostraram que enquanto o arsênio estava principalmente associado com oxi-hidróxidos de ferro nanoestruturados nas amostras de poeira inalável localizadas na região residencial da cidade de Paracatu, a arsenopirita era a principal fase de arsênio presente no minério. Este sulfeto concentra-se em partículas mais grosseiras no minério tratado, não sendo facilmente, pelo tamanho e elevada densidade, transportado via aérea.

Os resultados de arsênio bioacessível nos ensaios de bioacessibilidade pulmonar e gastrointestinal foram baixos (pulmão  $2,7 \pm 1\%$ ,  $n = 5$  e G.I  $3,4 \pm 2\%$ ,  $n = 14$ ) em áreas residenciais. As contribuições da máxima exposição (ingresso) por meio de inalação e por ingestão são pequenas (0,1% e 5,2%, respectivamente) quando comparadas ao ingresso total de arsênio (considerando a ingestão de alimentos e de água). O ingresso total, por sua vez, é  $<7\%$  do limite inferior da dose de referência da Organização das Nações Unidas para Agricultura e Alimentação (BMDL<sub>0.5</sub>) de  $3,0\mu\text{g}/\text{kg}$  de peso corporal por dia. Os valores baixos de bioacessibilidade mostram-se coerentes como as fases portadoras de arsênio. Esses achados são relevantes, pois esclarecem que a exposição por inalação ou ingestão de arsênio em região sob a influência da mineração de ouro pode ser classificada como de baixo risco.

O foco do presente estudo foi o arsênio, metaloide naturalmente presente na região. No entanto este estudo também possibilita abrir novas frentes de pesquisa que consideram a análise mais específica de outros elementos, encontrados durante as análises realizadas.

Como resultado deste trabalho foram geradas as seguintes publicações:

Ciminelli, V.S.T.; Delbem, I.D.; Freitas, E.; Morais, M.; Gasparon, M. Single-particle identification of trace arsenic constituents in environmental samples. (2018). In: 7th International Congress on Arsenic in the Environment (As2018): Environmental Arsenic in a Changing World, Beijing, China, Proceedings, p. 227-230, 2018.

Morais, M.A.; Gasparon, M.; Delbem, I.D.; Caldeira, C.L.; Freitas, E.T.F.; Ng, J.C.; Ciminelli, V. S.T. (2019). Gastric/lung bioaccessibility and identification of arsenic-bearing phases and sources of fine surface dust in a gold mining district. *Science of the Total Environment*, Vol. 689, p. 1244–1254.

## 6 REFERENCES

Abu-Allaban, M., Gillies, J. A., Gertler, A. W., Clayton, R., Proffitt, D. Tailpipe, resuspended road dust, and brake-wear emission factors from on-road vehicles. *Atmospheric Environment*, v.37, p.5283-5293, 2003.

Adamson, I. Y. R., Prieditis, H., Hedgecock, C., Vincent, R. Zinc is the toxic factor in the lung response to an atmospheric particulate sample. *Toxicology and Applied Pharmacology*, v.166, p111–119, 2000.

ATSDR – Agency for Toxic Substances and Disease Registry), 2005. Public Health Assessment – Guidance Manual (update). U. S. Department of Health and Human Services. Public Health Service, Atlanta, GA. [https://www.atsdr.cdc.gov/hac/PHAManual/PDFs/PHAGM\\_final1-27-05.pdf](https://www.atsdr.cdc.gov/hac/PHAManual/PDFs/PHAGM_final1-27-05.pdf) (accessed 29 October 2017).

ATSDR – Agency for Toxic Substances and Disease Registry. Toxicological Profile for Arsenic. U.S. Department of Health and Human Services. Atlanta, 499p, 2007.

Basha, S., Jhala, J., Thorat, R., Goel, S., Trivedi, R., Shah, K., Menon, G., Gaur P., Mody, K. and Jha, B. Assessment of heavy metal content in suspended particulate matter of coastal industrial town, Mithapur, Gujarat, India. *Atmospheric Research*, v.97, p.257-265, 2010.

Beak, D. G., Basta, N. T., Scheckel, K. G., Traina, S. J. Bioaccessibility of Arsenic(V) Bound to Ferrihydrite Using a Simulated Gastrointestinal System. *Environ. Sci. Technol.*, v.40, p.1364–1370, 2006.

Boisa, N., Elom, N., Dean, J. R., Deary, M. E., Bird, G., Entwistle, J. A. Development and application of an inhalation bioaccessibility method (IBM) for lead in the PM<sub>10</sub> size fraction of soil. *Environment International*, v.70, p.132-142, 2014.

BRASIL. Resolução CONAMA nº 420, de 28 de dezembro de 2009. Publicado no D.O.U nº 249, 30 dez. 2009, p81-84.

BRAZIL. Resolução CONAMA nº 491, de 19 de novembro de 2018. Publicado no D.O.U nº 223, 21 nov. 2018, p155-156.

Brotons, J. M., Díaz, A. R., Sarría, F. A., Serrato, F. B. Wind erosion on mining waste in southeast Spain. *Land Degradation & Development*, v.21, p.196-209, 2010.

Caboche, J., Esperanza, P., Bruno, M., Alleman, L. Y. Development of an in vitro method to estimate lung bioaccessibility of metals from atmospheric particles. *Journal of Environmental Monitoring*, v.13, p.621–630, 2011.

CETEM – Centro de Tecnologia Mineral: Ministério da Ciência e Tecnologia. Tratamento de Minérios; Caracterização Tecnológica de Minérios. 4.ed, Rio de Janeiro, p.55-109, 2004.

Ciminelli, V. S. T., Antônio, D. C., Caldeira, C. L., Freitas, E. T. F., Delbem, I. D., Fernandes, M. M., Gasparon, M., Ng, J. C. Low arsenic bioaccessibility by fixation in nanostructured iron (Hydr)oxides: Quantitative identification of As-bearing phases. *Journal of Hazardous Materials*, v.353, p.261-270, 2018.

Ciminelli, V. S. T., Gasparon, M., Ng, J. C., Silva, G. C., Caldeira, C. L. Dietary arsenic exposure in Brazil: The contribution of rice and beans. *Chemosphere*, v.168, p.996-1003, 2017.

Costa, D. L., Dreher, K. L. Bioavailable transition metals in particulate matter mediate cardiopulmonary injury in healthy and compromised animal models. *Environmental Health Perspectives*, v.105, p.1053–1060, 1997.

Csavina, J., Field, J., Taylor, M. P., Gao, S., Landázuri, A., Betterton, E. A., Sáez, A. E. A review on the importance of metals and metalloids in atmospheric dust and aerosol from mining operations. *Science of the Total Environment*, v.433, p58-73, 2012.

Davies, N. M, Feddah, M. R. A novel method for assessing dissolution of aerosol inhaler products, *Int. J. Pharm*, v. 255, n.1–2, p.175–187, 2003.

Diacomanolis, V., Ng, J.C., Noller, B.N. Development of mine site close-out criteria for arsenic and lead using a health risk approach. In: *Mine Closure 2007. Proceedings of the Second International Seminar on Mine Closure, 16-19 October 2007, Santiago, Chile.* Eds. Andy Fourie, Mark Tibbett, Jacques Wiertz. 191-198.

Drahota, P., Raus, K., Rychlíková, E., Rohovec, J. Bioaccessibility of As, Cu, Pb, and Zn in mine waste, urban soil, and road dust in the historical mining village of Kank, Czech Republic. *Environ Geochem Health*, v.40, 1495–1512, 2018.

Drysdale, M., Bjorklund, K. L., Jamieson, H. E., Weinstein, P., Cook, A., Watkins, R. T. Evaluating the respiratory bioaccessibility of nickel in soil through the use of a simulated lung fluid. *Environ Geochem Health*, v.34, p.279–288, 2012.

Duggan, M. J., Inskip, M. J., Rundle, S. A., Moorcroft, J. S. Lead in playground dust and on the hands of school children. *Science of the Total Environment*, v.44, p.65-79, 1985.

Dung, T. T. T., Golreihan, A., Vassilieva, E., Phung, N. K., Cappuyns, V., Swennen, R. Insights into solid phase characteristics and release of heavy metals and arsenic from industrial sludge via combined chemical, mineralogical, and microanalysis. *Environment Science Pollution*, v.22, p.2205-2218, 2015.

Ettler, V., Piantone, P., Touray, J. C. Mineralogical control on inorganic contaminant mobility in leachate from lead-zinc metallurgical slag: experimental approach and long-term assessment. *Mineral Mag.*, v.67, p.1269–1283, 2003.

EU – European Union. Directive 2004/107/EC of the European Parliament and of the Council. Official Journal of the European Union, L23/1-L23/16, Jan. 2005.

Fandrich, R. Gu, Y., Burrows, D., Moeller, K. Modern SEM-based mineral liberation analysis. *International Journal of Mineral Processing*, v.84, p.310-320, 2007.

Gamble, J. L. *Chemical anatomy, physiology, and pathology of extracellular fluid: A lecture syllabus*, 6th.ed., Cambridge: University of Michigan, 164p, 1941.

Gasparon, M., Delbem, I., Elmes, M., Ciminelli, V. S. T. Detection and analysis of arsenic-bearing particles in atmospheric dust using Mineral Liberation Analysis. In: *Arsenic Research and Global Sustainability, 6<sup>th</sup> International Congress on Arsenic in the environment – proceedings*. Stockholm, p.217–218, 2016.

Ghio, A. J., Stonehuerner, J., Dailey, L. A., Carter, J. D. Metals associated with both the water-soluble and insoluble fractions of an ambient air pollution particle catalyze an oxidative stress. *Inhalation Toxicology*, v.11, p37–49, 1999.

Gray, J. E., Plumlee, G. S., Morman, S. A., Higuera, P. L., Crock, J. G., Lowers, H. A., Witten, M. L. In Vitro Studies Evaluating Leaching of Mercury from Mine Waste Calcine Using Simulated Human Body Fluids. *Environmental Science Technology*, v.44, n.12, p.4782-4788, 2010.

Gu, Y. Automated Scanning Electron Microscope Based Mineral Liberation Analysis - An Introduction to JKMRC/FEI Mineral Liberation Analyser. *Journal of Minerals & Materials Characterization & Engineering*, v. 2, n.1, p.33-41, 2003.

Guilherme, L. R. G, Toujaguez, R., Ono, F. B., Martins, V. Arsenic speciation and bioaccessibility in gold mining tailings, Cuba. In: *Understanding the Geological and Medical Interface of Arsenic, 4<sup>th</sup>*, 2012, Cairns. *Arsenic in the environment –proceedings*. p.428–430.



Guney, M., Bourges, C., M.-J., Chapuis, R., P., Zagury, G., J. Lung bioaccessibility of As, Cu, Fe, Mn, Ni, Pb, and Zn in fine fraction (<20  $\mu\text{m}$ ) from contaminated soils and mine tailings. *Science of the Total Environment*, v.579, p.378–386, 2017.

Guney, M., Chapuis, R., P., Zagury, G., J. Lung bioaccessibility of contaminants in particulate matter of geological origin. *Environ Sci Pollut Res*, v.23, p.24422–24434, 2016.

Harmsen, J., Naidu, R. Bioavailability as a tool in site management. *Journal of Hazardous Materials*, v.261, p.840-846, 2013.

Heal, M. R., Hibbs, L. R., Agius, R. M., Beverland, I. J. Total and water-soluble trace metal content of urban background  $\text{PM}_{10}$ ,  $\text{PM}_{2.5}$  and black smoke in Edinburgh, UK. *Atmospheric Environment*, v. 39, p1417–1430, 2005.

Hettiarachchi, G. M., Pierzynski, G. M. Soil lead bioavailability and in situ remediation of lead-contaminated soils: a review. *Environmental Progress, New York*, v.23, n.1, p.78-93, 2004.

Hu, X., Zhang, W., Ding, Z., Wang, T., Lian H., Sun W., Wu, J. Bioaccessibility and health risk of arsenic and heavy metals (Cd, Co, Cr, Cu, Ni, Pb, Zn and Mn) in TSP and  $\text{PM}_{2.5}$  in Nanjing, China. *Atmospheric Environment*, v.57, p.146-152, 2012.

Huang, M., Chen, X., Zhao, Y., Chan, C., Y., Wang, W., Wang, X., Wong, M., H. Arsenic speciation in total contents and bioaccessible fractions in atmospheric particles related to human intakes. *Environmental Pollution*, v.188, p.37-44, 2014a.

Huang, M., Wang, W., Chan, C. Y, Cheung, K. C., Man, Y. B., Wang, X, Wong, M. H. Contamination and risk assessment (based on bioaccessibility via ingestion and inhalation) of metal(loid)s in outdoor and indoor particles from urban centers of Guangzhou, China. *Science of the Total Environment*, v.479–480, p.117–124, 2014b.

IARC – International Agency for Research on Cancer. Arsenic, metals, fibres, and dusts. Monographs on the evaluation of carcinogenic risks to humans. A review of human carcinogens, v.100 (C), Lyon, France, 2012.

IARC - International Agency for Research on Cancer. Outdoor air pollution a leading environmental cause of cancer deaths, Press Release n.221, Lyon, France, 2013.

IARC - International Agency for Research on Cancer. Some Drinking-water Disinfectants and Contaminants, including Arsenic: Monographs on the evaluation of Carcinogenic Risk to Humans, v.84, Lyon, France, 2004.

IBGE (Brazilian Institute of Geography and Statistics), 2015. Population estimation. [https://ww2.ibge.gov.br/home/estatistica/populacao/estimativa2015/estimativa\\_tcu.shtm](https://ww2.ibge.gov.br/home/estatistica/populacao/estimativa2015/estimativa_tcu.shtm) (accessed 12.01.18).

Jancsek-Turóczi, B., Hoffer, A., Nyíró-Kósa, I., Gelencsér, A. Sampling and characterization of resuspended and respirable road dust. *Journal of Aerosol Science*, v.65, p.69-76, 2013.

JECFA (Joint FAO/WHO Expert Committee on Food Additives). Evaluation of Certain Contaminants in Food. The seventy-second report, WHO, 1-115, 2011.

Juhasz, A. L., Smith, E. Weber, J., Rees, M., Rofe, A., Kuchel, T., Sansom, L. Naidu, R. In vitro assessment of arsenic bioaccessibility in contaminated (anthropogenic and geogenic) soils. *Chemosphere*, v.69, p.69-78, 2007.

Juhasz, A. L., Weber, J., Smith, E., Naidu, R., Marschner, B., Rees, M., Rofe, A., Kuchel, T., Sansom, L. Evaluation of SBRC-gastric and SBRC-intestinal methods for the prediction of in vivo relative lead bioavailability in contaminated soils. *Environmental Science and Technology*, v.43, p.4503-4509, 2009a.

Juhasz, A. L., Smith, E., Weber, J., Naidu, R., Rees, M., Rofe, A., Kuchel, T., Sansom, L. Assessment of four commonly employed in vitro arsenic bioaccessibility assays for predicting in vivo arsenic bioavailability in contaminated Soils. *Environmental Science and Technology*, v.43, p.9487-9494, 2009b.

Jurinski, J. B., Rimstidt, J. D. Biodurability of talc. *American Mineralogist*, Virginia, v.86, p392–399, 2001.

Kastury, F., Smith, E., Juhasz, A., L. A critical review of approaches and limitations of inhalation bioavailability and bioaccessibility of metal(loid)s from ambient particulate matter or dust. *Science of the Total Environment*, v.574, p.1054–1074, 2017.

Kelly, F. J., Fussell, J. C. Size, source and chemical composition as determinants of toxicity attributable to ambient particulate matter. *Atmospheric Environment*. V.60, p.504-526. 2012.

Keshavarzi, B., Moore, F., Rastmanesh, F., Kermani, M. Arsenic in Muteh gold mining district, Isfahan, Iran. *Environmental Earth Science*, v.67, p.959-970, 2012.

Kim, C. S., Anthony, T. L., Goldstein, D., Rytuba J. J. Windborne transport and surface enrichment of arsenic in semi-arid mining regions: Examples from the Mojave Desert, California. *Aeolian Research*, v.14, p.85–96, 2014.

Kim, J. Y., Kim, K. W., Lee, J. U., Lee, J. S., Cook, J. Assessment of As and heavy metal contamination in the vicinity of Duckum Au-Ag mine, Korea. *Environmental Geochemistry and Health*, v.24, p.215–227, 2001.

Li, Z., Ma, Z., Kuijp, T., J., Tsering, J., Yuan, Z., Huang, L. A review of soil heavy metal pollution from mines in China: Pollution and health risk assessment. *Science of the Total Environment*, v.468–469, p.843–853, 2014.

Marafante, E., Vahter, M. Solubility, retention and metabolism of intratracheally and orally administered inorganic arsenic compounds in the hamster. *Environ Res.*, v.42, p.72-82, 1987.

Martin, R., Dowling, K., Nankervis, S., Pearce, D., Florentine, S., McKnight, S. In vitro assessment of arsenic mobility in historical mine waste dust using simulated lung fluid. *Environ Geochem Health*, v. 40, p.1037–1049, 2018.

Mello, J.W.V., Roy, W.R., Talbott, J.L., Stucki, J.W. Mineralogy and Arsenic Mobility in Arsenic-rich Brazilian Soils and Sediments. *Journal of Soils and Sediments*, v. 6(1), p. 9–19, 2006.

Meunier, L., Walker, S. R., Wragg, J., Parsons, M. B., Koch, I., Jamieson, H. E. Effects of soil composition and mineralogy on the bioaccessibility of arsenic from tailings and soil in gold mine districts of Nova Scotia. *Environmental Science and Technology*, v.44, p.2667–2674, 2010.

Ng, J. C., Gasparon, M., Ciminelli, V. S. T., Oliveira, G. D. A. M., 2014. Health risk assessment of arsenic in residential area adjoining to a gold mine in Brazil. In: *One Century of the Discovery of Arsenicosis in Latin America (1914-2014)*, 5th International Congress on Arsenic in the environment – proceedings. Buenos Aires, p.602–604.

Ng, J. C., Juhasz, A. L., Smith, E., Naidu, R. Assessing the bioavailability and bioaccessibility of metals and metalloids. *Environmental Science Pollution Research*, v.22, p.8802-8825, 2015.

Ng, J. C., Juhasz, A. L., Smith, E., Naidu, R. Contaminant bioavailability and bioaccessibility: Part 1. Scientific and Technical Review. CRC CARE Technical Report 14. CRC for Contamination Assessment and Remediation of the Environment, Adelaide, Australia. 74 pp, 2010.

Niu, J., Rasmussen, P. E., Hassan, N. M., Vicent, R. Concentration Distribution and Bioaccessibility of Trace Elements in Nano and Fine Urban Airborne Particulate Matter: Influence of Particle Size. *Water Air Soil Pollut*, v.213, p211–225, 2010.

Ono, F. B., Guilherme, L. R. G., Penido, E. S., Carvalho, G. S., Hale, B., Toujaguez, R., Bundschuh, J. Arsenic bioaccessibility in a gold mining area: a health risk assessment for children. *Environ Geochem Health*, v.34, p457–465, 2012.

Ono, F. B., Tappero, R., Sparks, D., Guilherme, L. R. G. Investigation of arsenic species in tailings and windblown dust from a gold mining area. *Environ Sci Pollut Res*, v.23, p638–647, 2016.

Oomen, A. G., Hack, A., Minekus, M., Zeijdner, E., Cornelis, C., Schoeters, G., Verstraete, W., Wiele, T. V., Wragg, W., Rempelberg, C. J. M., Sips A. J. A. M., Wijnen, J. W. V. Comparison of Five In Vitro Digestion Models To Study the Bioaccessibility of Soil Contaminants. *Environ. Sci. Technol.*, v. 36, p.3326-3334, 2002.

Prieditis, H., Adamson, I. Y. R. Comparative pulmonary toxicity of various soluble metals found in urban particulate dust. *Experimental Lung Research*, v.28, p563–576, 2002.

Rezende, P. S., Costa, L. M., Windmoller, C. C. Arsenic Mobility in Sediments from Paracatu River Basin, MG, Brazil. *Arch Environ Contam Toxicol*, v.68, p.588–602, 2015.

Rhoads, K., Sanders C. L. Lung clearance, translocation and acute toxicity of arsenic, beryllium, cadmium, cobalt, lead, selenium, vanadium, and ytterbium oxides following deposition in rat lung. *Environmental Research*, v.36, p.359-378, 1985.

Ruby, M. V., Davis, A., Schoof, R., Eberle, S., Sellstone, C. M. Estimation of lead and arsenic bioavailability using a physiologically based extraction test. *Science of the Total Environment*, v.30, n.2, p422–430, 1996.

Ruby, M. V., Davis, A., Timothy, E. Link, T. E., Schoof, R., Chancy, R. L., Freeman, G. B., Bergstrom, P. Development of an in Vitro Screening Test To Evaluate the in Vivo Bioaccessibility of Ingested Mine-Waste Lead. *Environmental Science and Technology*, v.27, n.13, p.2870-2877, 1993.

Ruby, M. V., Schoof, R., Brattin, W., Goldade, M., Post, G., Harnois, M. Advances in evaluating the oral bioavailability of inorganics in soil for use in human health risk assessment. *Environmental Science and Technology*, v.33, p3697–3705, 1999.

Shaheen, N., Shah, M. H., Jaffar, M. A study of airborne selected metals and particle size distribution in relation to climatic variable and their source identification. *Water, Air and Soil Pollution*, v.164, p.275-294. 2005.

Toujaguez, R., Ono, F. B, Martins, V., Cabrera, P. P., Blanco, A. V., Bundschuh, Guilherme, L. R. G. Arsenic bioaccessibility in gold mine tailings of Delita, Cuba. *Journal of Hazardous Materials*, v.262, p.1004-1013, 2013.

USEPA – United States Environmental Protection Agency. 1995. Integrated Risk Information System (IRIS) National Center for Environmental Assessment. Arsenic, inorganic(CASRN-7440-38-2), [https://cfpub.epa.gov/ncea/iris/iris\\_documents/documents/subst/0278\\_summary.pdf](https://cfpub.epa.gov/ncea/iris/iris_documents/documents/subst/0278_summary.pdf), (accessed 16 July 2016).

USEPA – United States Environmental Protection Agency. 2015. Particulate Matter. <http://www.epa.gov/airquality/particulatematter/>. Accessed on September 05<sup>th</sup> of 2015.

USEPA – United States Environmental Protection Agency. 2016. Human Health Risk Assessment. <https://www.epa.gov/risk/human-health-risk-assessment>. Accessed on February 14<sup>th</sup> of 2019.

USEPA – United States Environmental Protection Agency. 2019. Terminology Services (TS). Terms and Acronyms. [https://iaspub.epa.gov/sor\\_internet/registry/termreg/searchandretrieve/termsandacronym/s/search.do](https://iaspub.epa.gov/sor_internet/registry/termreg/searchandretrieve/termsandacronym/s/search.do). Accessed on February 24<sup>th</sup> of 2019.

USEPA – United States Environmental Protection Agency. Compendium of ERT Waste Sampling Procedures. EPA/540/P-91/008 Oswer Directive 9360.4-07. Environmental Response Team – Emergency Response Division, Washington, DC, 1991.

USEPA – United States Environmental Protection Agency. Microwave assisted acid digestion of sediments, sludges, soils, and oils. Method 3051A, 2007.

USEPA – United States Environmental Protection Agency. Validation assessment of in vitro lead bioaccessibility assay for predicting relative bioavailability of lead in soils and soil-like materials at superfund sites. Oswer Directive 9200.3-51. United States Environment Protection Agency, Washington, DC, 2009.

Vahter, M. Environmental and occupational exposure to inorganic arsenic. *Acta Pharmacol Toxicol*, v.59, p.31-34, 1986.

Vodička, P., Smetana, K., Dvořánková, B., Emerick, T., Xu, Y. Z, Ourednik, J., Ourednik, V., Motlík, J. The Miniature Pig as an Animal Model in Biomedical Research. *Annals of the New York Academy of Sciences*, v.1049, p.161-171, 2005.

Wallenborn, J. G, McGee, J. K, Schladweiler, M. C, Ledbetter, .A. D., Kodavanti, U. P. Systemic translocation of particulate matter-associated metals following a single intratracheal instillation in rats. *Toxicol. Sci*, v.98, n.1, p.231–239, 2007.

WHO (World Health Organization). Arsenic in Drinking-water Background Document for Development of WHO Guidelines for Drinking-water Quality. WHO Press, World Health Organization, 20 Avenue Appia, 1211 Geneva 27, Switzerland, 2011.

Wiseman, C. L. S. Analytical methods for assessing metal bioaccessibility in airborne particulate matter: A scoping review. *Analytica Chimica Acta*, v.877, p.9-18, 2015.

Wiseman, C. L. S., Zereini, F. Characterizing metal(loid) solubility in airborne PM10, PM2.5 and PM1 in Frankfurt, Germany using simulated lung fluids. *Atmospheric Environment*, v.89, p.282–289, 2014.

Yager, J. W., Greene, T., Schoof R. A. Arsenic relative bioavailability from diet and airborne exposures: Implications for risk assessment. *Science of the Total Environment*, v.536, p.368–381, 2015.

Zheng, J., Huynh, T., Gasparon, M., Ng, J., Noller, B. Human health risk assessment of lead from mining activities at semi-arid locations in the context of total lead exposure. *Environmental Science Pollution Research*, v.20, p.8404-8416, 2013.

Zheng, Na., Liu, J., Wang, Q., Liang, Z. Health risk assessment of heavy metal exposure to street dust in the zinc smelting district, Northeast of China. *Science of the Total Environment*, v.408, p.726-733, 2010.